DALTON

Structure and dynamics of the η^2-hexafluorobenzene complexes $[Re(\eta^5\text{-}C_5H_4R)(CO)_2(\eta^2\text{-}C_6F_6)]$ (R = H or Me) and $[Rh(\eta^5\text{-}C_5Me_5)(PMe_3)(\eta^2\text{-}C_6F_6)]$

Catherine L. Higgitt,[a] A. Hugo Klahn,[b] Madeleine H. Moore,[a] Beatriz Oelckers,[b] Martin G. Partridge[a] and Robin N. Perutz*,[a]

[a] *Department of Chemistry, University of York, York YO1 5DD, UK*
[b] *Department of Chemistry, Universidad Catolica de Valparaiso, Casilla 4059 Valparaiso, Chile*

Photolysis of $[Re(\eta^5\text{-}C_5H_4R)(CO)_3]$ (R = H or Me) in hexafluorobenzene yielded $[Re(\eta^5\text{-}C_5H_4R)(CO)_2(\eta^2\text{-}C_6F_6)]$ containing the η^2-co-ordinated arene. The complex containing $\eta^5\text{-}C_5H_5$ has been characterised crystallographically. It forms monoclinic crystals in space group $P2_1/n$ with $Z = 4$, $a = 7.926(2)$, $b = 12.179(4)$, $c = 13.675(4)$ Å and $\beta = 102.91(2)°$. The structure reveals the expected features of distortion of the C_6F_6 unit from planarity at the co-ordinated C–C bond. The rhenium lies 2.059(7) Å from the mid-point of the co-ordinated C–C bond of C_6F_6. The IR and low-temperature ^{19}F NMR spectra reveal the presence of two rotamers, which are interconverted by rotation about the metal–C_6F_6 bond with $\Delta G^{\ddagger} = 36.7$ kJ mol^{-1} at 184 K. At higher temperatures a second intramolecular rearrangement causes broadening of the ^{19}F resonances. This fluxional process has been identified as a [1, 2]-shift of the site of rhenium co-ordination by linewidth and exchange spectroscopy measurements: $\Delta H^{\ddagger} = 57.6 \pm 0.5$ kJ mol^{-1}, $\Delta S^{\ddagger} = -7 \pm 2$ J K^{-1} mol^{-1}. The dynamic behaviour of the ($\eta^5\text{-}C_5H_4Me$) complex is extremely similar. The crystal structure of $[Rh(\eta^5\text{-}C_5Me_5)(PMe_3)(\eta^2\text{-}C_6F_6)]$, synthesised previously, has been determined for comparison. It crystallises in the same space group with $a = 8.694(9)$, $b = 16.818(9)$, $c = 14.642(6)$ Å and $\beta = 106.69(6)°$. The structural features of this rhodium complex are very similar to the rhenium complex, but the metal lies 1.920(5) Å from the mid-point of the co-ordinated C–C bond of the C_6F_6 unit. The shortening of the M–C_6F_6 bond is associated with the stereochemical rigidity of this complex. The C–F bonds of the co-ordinated carbons atoms are 0.049(7) Å longer than the remaining C–F bonds. Comparison of structural features of three $\eta^2\text{-}C_6F_6$ complexes revealed that the distortions of the C_6F_6 unit are almost constant, indicating a hard potential-energy surface. The analogy to co-ordinated C_2F_4 is reinforced by the similarity in co-ordination geometry. The electron-withdrawing character of $\eta^2\text{-}C_6F_6$ is confirmed by the $\tilde{\nu}$(CO) frequencies of $[Re(\eta^5\text{-}C_5H_5)(CO)_2(\eta^2\text{-}C_6F_6)]$ which lie at the high limit for complexes of the type $[Re(\eta^5\text{-}C_5H_5)(CO)_2L]$.

Although co-ordination of arenes through all six carbon atoms (η^6) remains the norm, the last few years have seen progress in stabilising structures in which the arene is co-ordinated through two or four carbon atoms (η^2 and η^4). Properties of such co-ordinated arenes are altered substantially from those of the free arene. Complexes with η^2-co-ordinated arenes play an important role in facilitating activation of arene C–H bonds.[1]

The first examples of η^2-arene complexes were reported in the 1960s[2] and the first example of an η^2-complex with a fused polycyclic arene was reported in 1977.[3] Prior to the studies by Harman and Taube[4–7] of $[Os(NH_3)_5(\eta^2\text{-arene})]^{2+}$ only a handful of η^2-arene complexes were known. Examination of the reactions of fused polycyclic aromatics has revealed the origin of the tendency to form η^2-complexes and provided examples of η^2-arene and aryl hydride complexes in equilibrium.[3,8–10]

The hapticity shift from η^6 to η^4 may play a key role in substitution reactions of arenes and be important in transition-metal catalysed hydrogenation of arenes but examples of η^4-arene complexes are limited.[11] Geiger and co-workers[12] have recently examined arene co-ordination in formally 19 e$^-$ Ru and Rh sandwich complexes and η^6 to η^4 hapticity changes of arenes induced by electron transfer. Co-ordination of C_6H_6 in the η^4-mode has been reported in a series of neutral and charged complexes: $[Cr(\eta^4\text{-}C_6H_6)(CO)_3]^{2-}$, $[Mn(\eta^4\text{-}C_6H_6)(CO)_3]^-$,[11,13,14] $[Ir\{MeC(CH_2PPh_2)_3\}(\eta^4\text{-}C_6H_6)]^+$,[15] $[Ir(\eta^5\text{-}C_5H_5)(\eta^4\text{-}C_6H_6)]$[16] and $[Rh(\eta^5\text{-}C_5H_5)(\eta^4\text{-}C_6H_6)]$.[17]

The scope of the co-ordination modes of C_6H_6 and other arenes has become apparent. Initially, arene co-ordination was observed principally for mononuclear complexes[18] but now many multinuclear complexes are known with bridging and capping arenes. Arenes which act as bridging ligands in multinuclear complexes serve as models for intermediate steps in arene-exchange reactions and for adsorbates on metal surfaces.[19–22] Many of these systems are highly fluxional and have been investigated by one- and two-dimensional NMR.[22,23]

We have shown that hexafluorobenzene is particularly effective as a ligand for η^2- and η^4-co-ordination at electron-rich metal centres. We have characterised $[Rh(\eta^5\text{-}C_5R_5)(PMe_3)(\eta^2\text{-}C_6F_6)]$,[24] $[Ir(\eta^5\text{-}C_5R_5)(C_2H_4)(\eta^2\text{-}C_6F_6)]$,[25] $[Ir(\eta^5\text{-}C_5H_5)(PMe_3)(\eta^2\text{-}C_6F_6)]$[24] and $[Ir(\eta^5\text{-}C_5R_5)(\eta^4\text{-}C_6F_6)]$[25] (R = H or Me). Timms and co-workers have shown that $\eta^6\text{-}C_6F_6$ and $\eta^4\text{-}C_6F_6$ complexes may be generated by metal vapour synthesis and have characterised a series of complexes $[W(\eta^6\text{-}C_6F_6)_2]$, $[M(\eta^6\text{-}C_6F_6)(\eta^6\text{-arene})]$ (M = Mo or W; arene = C_6H_6, $C_6H_3F_3$-1,3,5 or $C_6H_3Me_3$-1,3,5)[26] and $[M(\eta^4\text{-}C_6F_6)(\eta^6\text{-arene})]$ (M = Ru or Os; arene = $C_6H_3Me_3$-1,3,5, $C_6H_4Me_2$-1,3 or C_6H_6).[27]

A number of alternative types of reactions of hexafluorobenzene at transition-metal centres have been documented. Hexafluorobenzene may act as a one-electron oxidising agent as with $[Cr(\eta^6\text{-}C_6H_6)_2]$,[28] or may undergo oxidative addition. The direct product of oxidative addition is expected to be of the type $M(C_6F_5)F$ and is observed on irradiation of $[Rh(\eta^5\text{-}C_5Me_5)(PMe_3)(\eta^2\text{-}C_6F_6)]$[24] or on thermal reaction of [PtH(dbpm)(CH_2CMe_3)] (dbpm = $Bu^t_2PCH_2PBu^t_2$) with C_6F_6.[29] However, metal dihydrides react with the elimination of HF yielding $M(C_6F_5)H$ complexes.[24,30] Elimination of HF also provides the driving force for the reaction of $[Re(\eta^5\text{-}C_5Me_5)(CO)_3]$ with C_6F_6 to form $[Re(\eta^6\text{-}C_5Me_4CH_2)Re(CO)_2(C_6F_5)]$.[31] Homogeneous

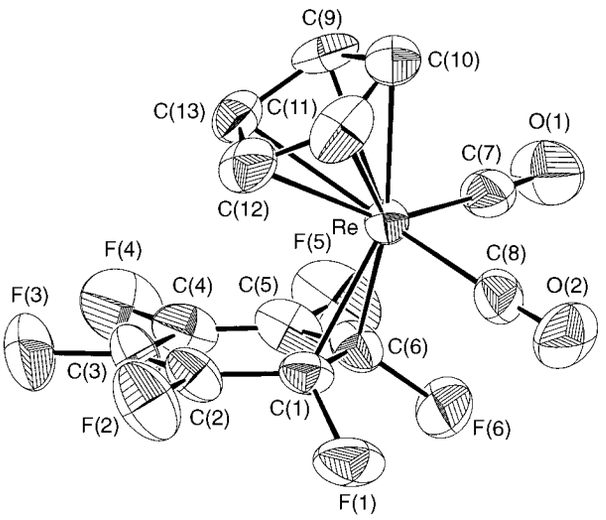

Fig. 1 An ORTEP[35] diagram (50% thermal ellipsoids) of [Re(η^5-C_5H_5)(CO)$_2$(η^2-C_6F_6)]

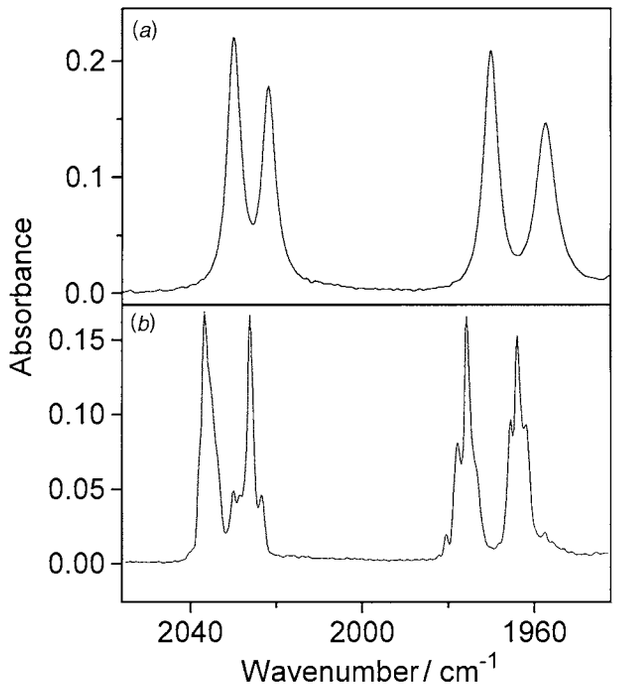

Fig. 2 Infrared spectra of [Re(η^5-C_5H_5)(CO)$_2$(η^2-C_6F_6)] (*a*) in hexane solution at 298 K, (*b*) in argon matrix at 12 K

catalytic conversion of C_6F_6 to C_6F_5H has recently been achieved with a rhodium complex.[32] Kiplinger and Richmond[33] report selective room-temperature hydrogenolysis of aromatic C–F bonds using a low-valent zirconocene species. The reactions of C_6F_6 with a variety of transition-metal complexes have been reviewed recently.[34]

The molecular structures of [Rh(η^5-C_5H_5)(PMe_3)(η^2-C_6F_6)][24] and [Ir(η^5-C_5H_5)(C_2H_4)(η^2-C_6F_6)][25] both show that the two fluorine atoms bonded to the co-ordinated carbon atoms are no longer co-planar with the remaining C_6F_4 moiety. The C–C bonds of the C_6F_6 unit are distorted so that the ligand contains a co-ordinated C–C bond and unco-ordinated diene unit. The M(η^2-C_6F_6) complexes characterised so far have proved to be stereochemically rigid on the NMR timescale. However, [Ir(η^5-C_5R_5)(C_2H_4)(η^2-C_6F_6)] (R = H or Me) is present as two isomers, assigned as the species related by rotation of C_6F_6 about the Ir–C_6F_6 bond.[25] The rate of interconversion of the isomers is slow compared to the NMR relaxation time.

In this paper, we report the syntheses of [Re(η^5-C_5H_4R)(CO)$_2$(η^2-C_6F_6)] (R = H or Me) and the crystal structure of the η^5-C_5H_5 complex. We show that these molecules are stereochemically non-rigid, undergoing two types of intramolecular rearrangement. We also report the crystal structure of [Rh(η^5-C_5Me_5)(PMe_3)(η^2-C_6F_6)], which proves to be free of the disorder which reduced the value of the structure of the η^5-C_5H_5 analogue.[24] Comparison of three structures containing η^2-co-ordinated C_6F_6 rings shows very little variation in geometric parameters. Finally, we assess the electronic characteristics of hexafluorobenzene as a ligand.

Results

Syntheses of [Re(η^5-C_5H_4R)(CO)$_2$(η^2-C_6F_6)] (R = H or Me)

The irradiation of [Re(η^5-C_5H_5)(CO)$_3$] in C_6F_6 ($\lambda > 315$ nm for 15 h) generates a single product identified as [Re(η^5-C_5H_5)(CO)$_2$(η^2-C_6F_6)]. The complex [Re(η^5-C_5H_4Me)(CO)$_2$(η^2-C_6F_6)] is prepared *via* a similar route.

Crystal and molecular structure of [Re(η^5-C_5H_5)(CO)$_2$(η^2-C_6F_6)]

The crystal structure of [Re(η^5-C_5H_5)(CO)$_2$(η^2-C_6F_6)] shows the same features that have proved characteristic of other η^2-hexafluorobenzene complexes (Fig. 1, Table 1).[24,25] The hexafluorobenzene ligand is folded at the co-ordinated C–C bond, C(1)–C(6). The atoms of the C_6F_4 unit, C(1)–C(6) and F(2)–F(5) are almost coplanar (r.m.s. deviation 0.020 Å) and tipped towards the C_5H_5 ring. The atoms C(1), C(6), F(1) and F(6) form the second plane, bent at 44.4(2)° to the first, and lying adjacent to the carbonyl groups. The angle between the C_6F_4 and the C_5H_5 planes is 31.3(3)°. The Re atom lies at 2.059(7) Å from the mid-point of C(1)–C(6) [labelled D(2)] and 1.947 Å from the centroid of the C_5H_5 ring [labelled D(1)]. The D(1)–Re–D(2) angle is 129.7°. Further details of the structure will be examined in the discussion.

Infrared studies of [Re(η^5-C_5H_4R)(CO)$_2$(η^2-C_6F_6)] (R = H or Me)

The IR spectrum of [Re(η^5-C_5H_5)(CO)$_2$(η^2-C_6F_6)] [Fig. 2(*a*)] recorded in hexane at room temperature shows two pairs of bands at 2030 and 1970 cm^{-1} and at 2022 and 1957 cm^{-1}, which are assigned to two isomeric forms of the product. The isomers are present in the approximate ratio of 1.3:1. Similarly, [Re(η^5-C_5H_4Me)(CO)$_2$(η^2-C_6F_6)] shows bands at 2026, 2019, 1966 and 1954 cm^{-1} in the same solvent. It proved impossible to discover the effect of altering the solvent on the isomer ratio for [Re(η^5-C_5H_4R)(CO)$_2$(η^2-C_6F_6)] as the IR bands were very broad in more polar solvents. Instead, IR spectra of [Re(η^5-C_5H_5)(CO)$_2$(η^2-C_6F_6)] were recorded in hexane at a series of temperatures down to 213 K. At 213 K the ratio had altered to 1:1. The IR spectrum was also investigated in an argon matrix. The vapour of a sample at 323 K was condensed with argon onto a window at 20 K, which was then cooled to 12 K. The spectrum of [Re(η^5-C_5H_5)(CO)$_2$(η^2-C_6F_6)] again shows four bands at 2037, 2026, 1976 and 1964 cm^{-1} although each is split into multiple components by matrix effects [Fig. 2(*b*)]. Thus in an Ar matrix there are still two isomeric forms present in a similar ratio to that seen at room temperature in solution. This ratio is likely to reflect the ratio of isomers present in the vapour prior to deposition.

On the basis of the IR data alone we deduce that [Re(η^5-C_5H_5)(CO)$_2$(η^2-C_6F_6)] exists as the two rotamers [shown in equation (1)] as seen for [Ir(η^5-C_5R_5)(C_2H_4)(η^2-C_6F_6)].[25] The

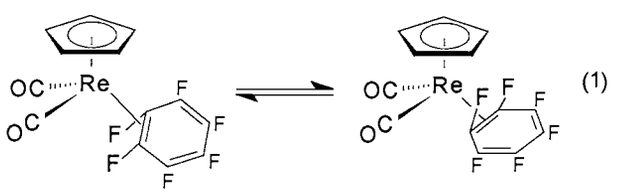

(1)

Table 1 Bond lengths (Å) and angles (°) for [Re(η^5-C_5H_5)(CO)$_2$(η^2-C_6F_6)] with estimated standard deviations (e.s.d.s) in the least significant figure(s) in parentheses

Re–C(8)	1.908(9)	O(1)–C(7)	1.155(11)
Re–C(7)	1.914(9)	O(2)–C(8)	1.150(11)
Re–C(1)	2.165(7)	C(1)–C(2)	1.418(11)
Re–C(6)	2.205(7)	C(1)–C(6)	1.476(12)
Re–C(10)	2.256(7)	C(2)–C(3)	1.337(12)
Re–C(9)	2.267(7)	C(3)–C(4)	1.430(13)
Re–C(11)	2.289(7)	C(4)–C(5)	1.313(13)
Re–C(12)	2.307(7)	C(5)–C(6)	1.442(13)
Re–C(13)	2.307(8)	C(9)–C(13)	1.383(13)
F(1)–C(1)	1.395(9)	C(9)–C(10)	1.431(14)
F(2)–C(2)	1.332(10)	C(10)–C(11)	1.415(14)
F(3)–C(3)	1.332(11)	C(11)–C(12)	1.383(12)
F(4)–C(4)	1.341(10)	C(12)–C(13)	1.424(14)
F(5)–C(5)	1.337(10)		
F(6)–C(6)	1.383(10)		
C(8)–Re–C(7)	86.5(4)	F(1)–C(1)–Re	118.9(5)
C(8)–Re–C(1)	87.3(3)	C(2)–C(1)–Re	118.4(6)
C(7)–Re–C(1)	113.9(3)	C(6)–C(1)–Re	71.7(4)
C(8)–Re–C(6)	95.3(3)	F(2)–C(2)–C(3)	120.2(8)
C(7)–Re–C(6)	75.9(3)	F(2)–C(2)–C(1)	117.4(8)
C(1)–Re–C(6)	39.5(3)	C(3)–C(2)–C(1)	122.4(8)
C(8)–Re–C(10)	102.7(3)	F(3)–C(3)–C(2)	122.7(8)
C(7)–Re–C(10)	97.0(3)	F(3)–C(3)–C(4)	116.5(8)
C(1)–Re–C(10)	148.2(3)	C(2)–C(3)–C(4)	120.8(9)
C(6)–Re–C(10)	160.3(3)	C(5)–C(4)–F(4)	121.2(9)
C(8)–Re–C(9)	138.5(3)	C(5)–C(4)–C(3)	121.0(8)
C(7)–Re–C(9)	89.8(3)	F(4)–C(4)–C(3)	117.8(9)
C(1)–Re–C(9)	131.1(3)	C(4)–C(5)–F(5)	121.8(9)
C(6)–Re–C(9)	123.8(3)	C(4)–C(5)–C(6)	120.9(8)
C(10)–Re–C(9)	36.9(4)	F(5)–C(5)–C(6)	117.2(9)
C(8)–Re–C(11)	92.9(3)	F(6)–C(6)–C(5)	111.4(7)
C(7)–Re–C(11)	131.8(4)	F(6)–C(6)–C(1)	115.5(7)
C(1)–Re–C(11)	114.2(3)	C(5)–C(6)–C(1)	118.6(8)
C(6)–Re–C(11)	151.6(3)	F(6)–C(6)–Re	115.2(5)
C(10)–Re–C(11)	36.3(4)	C(5)–C(6)–Re	121.4(6)
C(9)–Re–C(11)	60.1(4)	C(1)–C(6)–Re	68.8(4)
C(8)–Re–C(12)	116.2(4)	O(1)–C(7)–Re	177.6(8)
C(7)–Re–C(12)	149.5(3)	O(2)–C(8)–Re	174.1(7)
C(1)–Re–C(12)	88.5(3)	C(13)–C(9)–C(10)	108.1(8)
C(6)–Re–C(12)	118.7(3)	C(13)–C(9)–Re	74.0(5)
C(10)–Re–C(12)	59.9(3)	C(10)–C(9)–Re	71.1(4)
C(9)–Re–C(12)	59.7(3)	C(11)–C(10)–C(9)	106.7(9)
C(11)–Re–C(12)	35.0(3)	C(11)–C(10)–Re	73.1(5)
C(8)–Re–C(13)	151.0(3)	C(9)–C(10)–Re	72.0(4)
C(7)–Re–C(13)	116.8(3)	C(12)–C(11)–C(10)	109.0(8)
C(1)–Re–C(13)	97.4(3)	C(12)–C(11)–Re	73.2(4)
C(6)–Re–C(13)	106.5(3)	C(10)–C(11)–Re	70.6(4)
C(10)–Re–C(13)	59.9(3)	C(11)–C(12)–C(13)	107.7(8)
C(9)–Re–C(13)	35.2(3)	C(11)–C(12)–Re	71.8(4)
C(11)–Re–C(13)	59.1(3)	C(13)–C(12)–Re	72.0(4)
C(12)–Re–C(13)	36.0(3)	C(9)–C(13)–C(12)	108.4(8)
F(1)–C(1)–C(2)	111.5(7)	C(9)–C(13)–Re	70.8(5)
F(1)–C(1)–C(6)	114.9(7)	C(12)–C(13)–Re	72.0(4)
C(2)–C(1)–C(6)	116.2(7)		

enthalpy change, $|\Delta H^{\ddagger}|$, for the interconversion of the rotamers is *ca.* 1.5 kJ mol^{-1} and the free energy change, $|\Delta G^{\ddagger}_{300}| \approx 0.7$ kJ mol^{-1}.

Variable-temperature ^{19}F NMR studies of [Re(η^5-C_5H_4R)(CO)$_2$(η^2-C_6F_6)] (R = H or Me)

The ^{19}F NMR (470 MHz) spectrum of [Re(η^5-C_5H_5)(CO)$_2$(η^2-C_6F_6)] in [$^2H_8$]thf shows three broad resonances at 301.5 K (figures in parentheses are the full widths at half maximum, f.w.h.m.): δ −144.2 (189), −151.5 (106) and −171.7 (94 Hz). On warming from 301.5 to 322 K the three resonances broaden further. The resonance at δ −144 broadens at approximately twice the rate of the other two resonances.

On cooling, the spectrum sharpens and at 280 K fine structure starts to appear in each resonance (Fig. 3). At 254.5 K there is optimum resolution of the fine structure (Fig. 4). Comparison with a ^{19}F NMR spectrum at 253 K recorded at 84.57 MHz shows that the fine structure of the resonance at δ −151.5 arises from *J* coupling of a single isomer rather than two isomers (the major splitting is 28 Hz at both field strengths). Nevertheless, on further cooling to 173 K, each resonance of the 470 MHz spectrum of [Re(η^5-C_5H_5)(CO)$_2$(η^2-C_6F_6)] starts to broaden again. The resonance at δ −151.5 broadens faster than the other two, reaching a f.w.h.m. of 76 Hz at 186 K (compared to 63 Hz for the δ −144 resonance and 58 Hz for the δ −171 resonance). At 186 K the coalescence point for the δ −151.5 resonance is reached and below this temperature this resonance splits into two signals at δ −150.90 and −150.85 (Fig. 5).

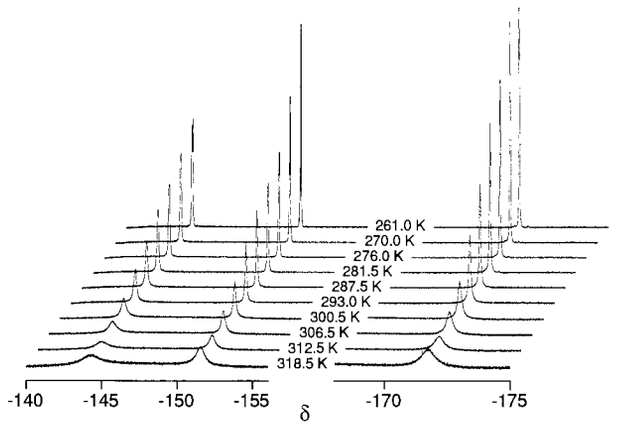

Fig. 3 Fluorine-19 NMR spectra of [Re(η^5-C_5H_5)(CO)$_2$(η^2-C_6F_6)] in [$^2H_8$]thf in the temperature range 320–260 K

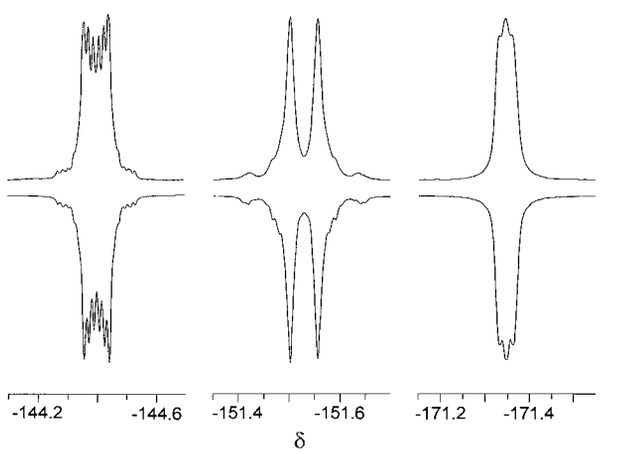

Fig. 4 Fluorine-19 NMR spectrum of [Re(η^5-C_5H_5)(CO)$_2$(η^2-C_6F_6)] in [$^2H_8$]thf at 254.5 K. Top observed and bottom simulated spectrum

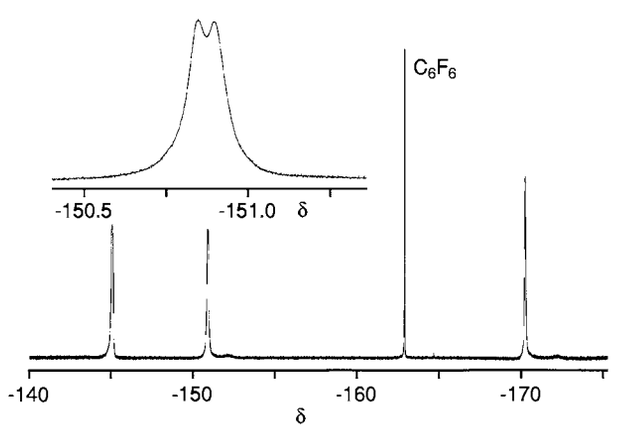

Fig. 5 Fluorine-19 NMR spectrum of [Re(η^5-C_5H_5)(CO)$_2$(η^2-C_6F_6)] in [$^2H_8$]thf at 178.5 K showing splitting of the δ −151 resonance (inset)

In all the samples there are traces of free C_6F_6 {ratio of $[Re(\eta^5\text{-}C_5H_5)(CO)_2(\eta^2\text{-}C_6F_6)]$:$C_6F_6$ ≈ 25:1}. The linewidth of the C_6F_6 resonance at δ −162.9 (f.w.h.m. = 2–3 Hz) does not alter over the temperature range explored.

The ^{19}F NMR spectrum of $[Re(\eta^5\text{-}C_5H_4Me)(CO)_2(\eta^2\text{-}C_6F_6)]$ in $[^2H_8]$thf is similar to that of $[Re(\eta^5\text{-}C_5H_5)(CO)_2(\eta^2\text{-}C_6F_6)]$. At 302.5 K three broad resonances are detected: δ −144.2 (f.w.h.m. = 193), −152.2 (f.w.h.m. = 103) and −172.0 (f.w.h.m. = 93 Hz). Again, the resonances sharpen on cooling, reaching an optimum at 257 K, before broadening on cooling further. Again, the spectrum at 257 K seems to indicate the presence of one isomeric species. For $[Re(\eta^5\text{-}C_5H_4Me)(CO)_2(\eta^2\text{-}C_6F_6)]$ the coalescence point for the δ −152 resonance is reached at 184 K and below this temperature the resonance splits again into two at δ −150.55 and −150.60.

^{19}F–^{19}F EXSY studies of $[Re(\eta^5\text{-}C_5H_4R)(CO)_2(\eta^2\text{-}C_6F_6)]$ (R = H or Me)

Exchange spectroscopy (EXSY)[36–38] is a suitable method for investigating slow exchange processes and determining the rates of exchange. At about 240 K the longitudinal relaxation times, T_1, of the three pairs of ^{19}F nuclei of $[Re(\eta^5\text{-}C_5H_5)(CO)_2(\eta^2\text{-}C_6F_6)]$ are approximately equal (T_1 ≈ 500–600 ms measured by inversion-recovery sequence). Thus $[Re(\eta^5\text{-}C_5H_5)(CO)_2(\eta^2\text{-}C_6F_6)]$ is amenable to study by EXSY at these temperatures using a simplified approach to data analysis (see below). The ^{19}F–^{19}F EXSY spectra of $[Re(\eta^5\text{-}C_5H_5)(CO)_2(\eta^2\text{-}C_6F_6)]$ in $[^2H_8]$thf were recorded at 236.5 and 243.5 K with mixing times, τ_m, of 50, 100, 150 and 500 ms (470.4 MHz). Pure two-dimensional absorption lineshapes were recorded through the use of suitable phase cycling. The EXSY spectra show intense cross-peaks linking sites F_a to F_m and F_m to F_x and a less intense cross-peak linking sites F_a to F_x (approximately 80 times less intense at the lowest temperature with the shortest mixing time). No cross-peaks are seen to the free C_6F_6 resonance. Fig. 6 shows one-dimensional sections from the EXSY spectrum at

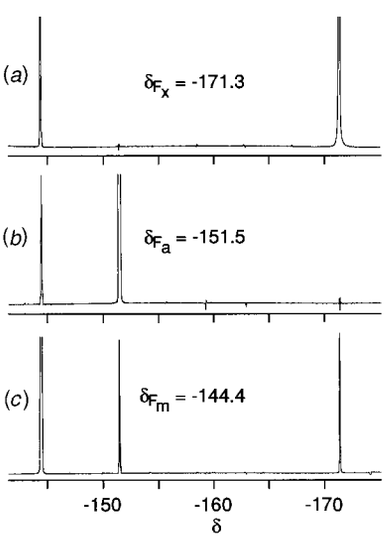

Fig. 6 One-dimensional sections at the frequencies of (*a*) F_x (δ −171.3), (*b*) F_a (δ −151.5) and (*c*) F_m (δ −144.4) from the ^{19}F–^{19}F EXSY spectrum of $[Re(\eta^5\text{-}C_5H_5)(CO)_2(\eta^2\text{-}C_6F_6)]$ in $[^2H_8]$thf at 243.5 K (τ_m = 50 ms) (note the absence of F_aF_x cross-peaks)

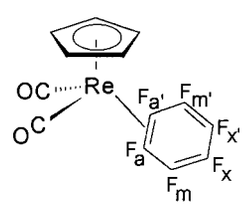

Table 2 Fluorine-19 chemical shifts and ^{19}F–^{19}F coupling constants obtained by simulation for $[Re(\eta^5\text{-}C_5H_5)(CO)_2(\eta^2\text{-}C_6F_6)]$ in $[^2H_8]$thf

δ	*J*/Hz	*J*/Hz	*J*/Hz
δ_A = −151.5	J_{AM} = 36.5	$J_{AX'}$ = 0.9	$J_{AA'}$ = 25.6
δ_M = −144.4	$J_{AM'}$ = −11.0	J_{MX} = 13.8	$J_{MM'}$ = 18.1
δ_X = −171.3	J_{AX} = 4.0	$J_{MX'}$ = 3.0	$J_{XX'}$ = 13.7

the frequencies of F_a, F_m and F_x. Similar results were obtained for $[Re(\eta^5\text{-}C_5H_4Me)(CO)_2(\eta^2\text{-}C_6F_6)]$ in $[^2H_8]$thf at 237.0 and 243.5 K (τ_m = 50, 100 and 150 ms).

Analysis of the dynamics of $[Re(\eta^5\text{-}C_5H_4R)(CO)_2(\eta^2\text{-}C_6F_6)]$ (R = H or Me)

At 300 K three broad singlets are seen in the ^{19}F NMR spectrum of $[Re(\eta^5\text{-}C_5H_5)(CO)_2(\eta^2\text{-}C_6F_6)]$. The sharp resonances of free C_6F_6 and the lack of cross-peaks to C_6F_6 in the EXSY spectra both indicate that there is no intermolecular exchange. On cooling, fine structure starts to appear for each resonance, reaching optimum resolution at 254.5 K. The symmetrical patterns which also appear in spectra run on a lower field instrument indicate that the fine structure results from F–F coupling. Simulation of the second-order effects in this $[AMX]_2$ spin system yields the couplings listed in Table 2 which must correspond to the averaged spectrum for the two rotamers identified from the IR.

The EXSY spectra indicate that the three pairs of fluorine nuclei undergo intramolecular chemical exchange. The intensities of the EXSY cross-peaks are consistent with the whizzing process shown below in which the point of attachment of the metal to the C_6F_6 ring undergoes a [1,2]-shift. As expected the relative intensity of the F_a to F_x cross-peak increases as the mixing time and temperature are increased (probably due to multiple [1,2] hops). Further evidence for this [1,2]-shift comes from the observation that the δ −144 resonance broadens at twice the rate of the other two resonances in the 300–322 K region. In Scheme 1, only one of the two A nuclei changes chemical shift at each step, only one of the X nuclei changes but both of the M nuclei change chemical shift. This effect adds an independent method of assigning the δ −144 resonance to F_m. If a [1,3]-shift occurred as the dominant process, all the resonances should broaden at the same rate.[39]

Since the spectra at 250 K are consistent with the presence of a single species, they are in the high-temperature limit of the Re–C_6F_6 rotation, but in the slow exchange region for ring-whizzing throughout the temperature range 250–320 K. Analysis of the bandwidths of the three fluorine resonances between 298.5 and 318.5 K was carried out to determine the rate and the activation parameters for this 'ring-whizzing' process. This temperature region was chosen as fine structure arising from F–F coupling makes a very small contribution to the linewidth. The spectra for $[Re(\eta^5\text{-}C_5H_4Me)(CO)_2(\eta^2\text{-}C_6F_6)]$ over the temperature range 297.5–325.0 K can be analysed in a similar way. The rate constant for exchange was determined from equation (2)

$$k_{whizz} = \pi(w_{\frac{1}{2}} - w_{0\frac{1}{2}}) \quad (2)$$

where k_{whizz} = rate constant of dynamic process at temperature *T* (averaged over the three resonances); $w_{\frac{1}{2}}$ = f.w.h.m. (Hz) of the resonance at the temperature *T* [take $w_{\frac{1}{2}}$ as equal to 0.5 f.w.h.m. (Hz) for the δ −144 resonance]; $w_{0\frac{1}{2}}$ = natural f.w.h.m. (Hz) of the resonance before exchange broadening sets in {best fit achieved when set to 5.0 Hz for $[Re(\eta^5\text{-}C_5H_5)(CO)_2(\eta^2\text{-}C_6F_6)]$ and 10.0 Hz for $[Re(\eta^5\text{-}C_5H_4Me)(CO)_2(\eta^2\text{-}C_6F_6)]$}. Fig. 7(*a*) shows the rate constant for ring-whizzing, k_{whizz}, *versus* temperature, *T*, for $[Re(\eta^5\text{-}C_5H_4R)(CO)_2(\eta^2\text{-}C_6F_6)]$ (R = H or Me) in $[^2H_8]$thf (Table 3).

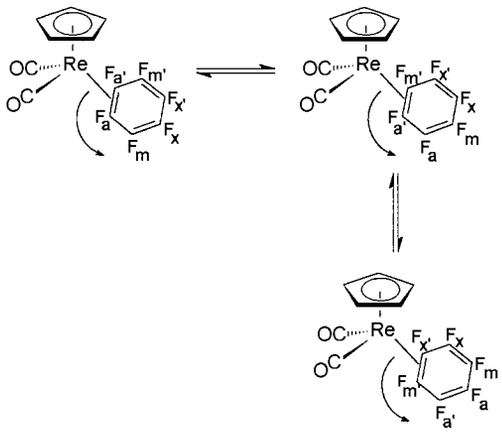

Scheme 1

Values of the rate constant for ring-whizzing, k_{whizz}, at lower temperatures were determined by analysis of the EXSY spectra. Cross-peaks in the spectra arise from chemical exchange. Appropriate phase cycling was used to suppress unwanted signals arising from coherent phenomena such as relayed magnetisation and single- and multiple-quantum coherence transfer processes.†[37,38] If cross-relaxation effects are neglected, the relationship between the cross-peak intensities, I_{ij}, and the first-order rate constant for chemical exchange from site i to site j, k_{ij}, may be written as shown in equation (3) (adapted from

$$I_{ij}(\tau_m) = (e^{-\mathbf{R}\tau_m})_{ij} M_j^\circ \quad (3)$$

Macura and Ernst)[38,40–42] where M_j° = equilibrium magnetisation of the nuclei in site j (intensity of the on-diagonal peak in site j when $\tau_m = 0$); **R** = relaxation matrix which comprises contributions from cross relaxation, spin–lattice relaxation and chemical exchange. The matrix has off-diagonal elements $\mathbf{R}_{ji} = -k_{ij}$.

The values of M_j° were determined with τ_m of 1 ms. For this system, M_j° is equal for each site j. By including M_j° values in the calculation, values for the spin–lattice relaxation rate for the nucleus in the jth site can be determined in addition to k_{ij}.[40]

For general multiple-site exchange equation (3) cannot be solved analytically. However, if sufficiently short mixing times are used, approximate solutions can be found by invoking the initial rate approximation given in equation (4). If τ_m is

$$e^{-\mathbf{R}\tau_m} \approx 1 + \mathbf{R}\tau_m \quad (4)$$

increased, it is necessary to include higher terms of the expansion of $e^{-\mathbf{R}\tau_m}$ to take account of multiple [1,2] hop processes. The rate constant for the [1,2]-shift process for [Re(η^5-C_5H_5)(CO)$_2$(η^2-C_6F_6)] was calculated using the initial rate approximation to be 0.38 ± 0.03 s^{-1} at 236.5 K and 1.01 ± 0.03 s^{-1} at 243.5 K. For a direct [1,3]-shift the rate was calculated to be some 600 times slower at 243.5 K. For [Re(η^5-C_5H_4Me)(CO)$_2$(η^2-C_6F_6)] the EXSY spectra yielded rate constants for the [1,2]-shift process of 0.37 ± 0.05 s^{-1} at 237.0 K and 0.98 ± 0.06 s^{-1} at 243.5 K. The rate of the [1,3]-shift process was again much slower.‡

Combination of the high-temperature rate constant data determined from linewidth analysis with the low-temperature data from the EXSY experiments allows the activation parameters for the 'ring-whizzing' process to be calculated. The Eyring plot of ln[k_{whizz}/T] *versus* 1/T [Fig. 7(*b*)] yields the activation parameters in Table 4. Rate data at intermediate temperatures are difficult to determine because of the complicating

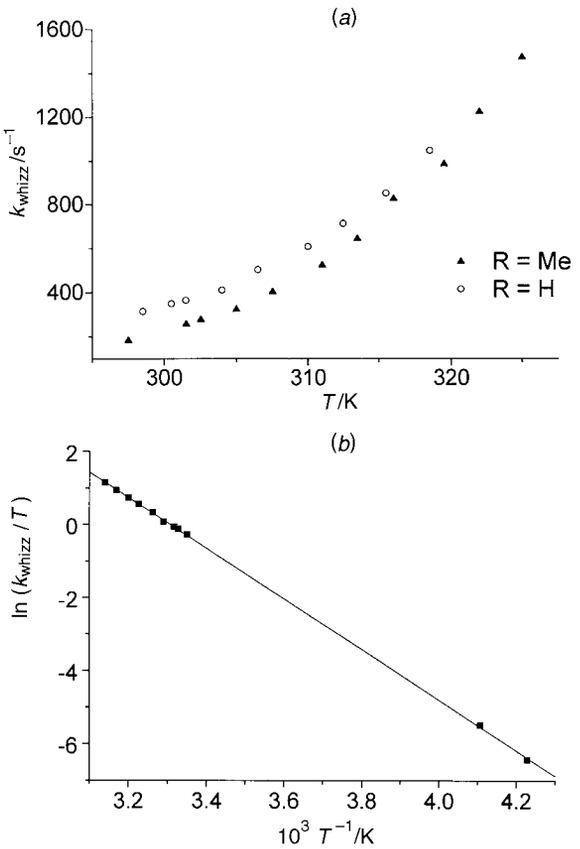

Fig. 7 (*a*) Rate constant for ring whizzing, k_{whizz}, *versus* temperature, T, for [Re(η^5-C_5H_4R)(CO)$_2$(η^2-C_6F_6)] (R = H ○ or Me ▲). (*b*) Eyring plot: ln(k_{whizz}/T) *versus* 1/T for [Re(η^5-C_5H_5)(CO)$_2$(η^2-C_6F_6)]

Table 3 Rate constants for ring-whizzing, k_{whizz}, at given temperatures for [Re(η^5-C_5H_4R)(CO)$_2$(η^2-C_6F_6)] (R = H or Me) in [$^2H_8$]thf

R = H		R = Me	
T/K	k_{whizz}/s^{-1}	T/K	k_{whizz}/s^{-1}
236.5	0.380	237.0	0.370
243.5	1.01	243.5	0.980
298.5	230	297.5	182
300.5	267	301.5	256
301.5	283	302.5	277
304.0	332	305.0	324
306.5	432	307.5	403
310.0	545	311.0	526
312.5	657	313.5	645
315.5	806	316.0	828
318.5	1010	319.5	988
		322.0	1230
		325.0	1480

† In coupled spin systems, zero-quantum coherence and longitudinal scalar or dipolar order can also give rise to cross-peaks (referred to as '*J* cross-peaks') that cannot be removed by phase cycling.[37,38] Longitudinal scalar or dipolar order effects can be minimised by careful calibration of π/2 pulses. The '*J* cross-peak' contributions to cross-peak intensities are shown to be negligible by the low intensity of the cross-peak linking the *J*–*J* coupled sites F_a to F_x. The amplitudes of '*J* cross-peaks' show a sinusoidal (dampened) dependence on τ_m while the amplitudes of exchange cross-peaks rapidly increase (due to exchange) and then slowly decay away (due to spin-lattice relaxation) as τ_m increases. The value of the rate constant for the [1,2]-shift process was found to be invariant (within experimental error) with mixing time over the region investigated. This observation gives further support to the assumption that the contribution to cross-peak intensities from '*J* cross-peaks' is negligible.

‡ At *ca.* 240 K, the exchange rate of *ca.* 0.8 s^{-1} is slightly slower than the inverse relaxation time, $T_1^{-1} \approx 2$ s^{-1}.

Table 4 Activation parameters for ring-whizzing and propeller rotation in $[Re(\eta^5\text{-}C_5H_4R)(CO)_2(\eta^2\text{-}C_6F_6)]$ (R = H or Me)

	Ring whizzing				Propeller rotation
R	$\Delta H^{\ddagger}$/ kJ mol^{-1}	$\Delta S^{\ddagger}$/ J K^{-1} mol^{-1}	$\Delta G^{\ddagger}_{300}$/ kJ mol^{-1}	$\Delta G^{\ddagger}_{186}$ / kJ mol^{-1}	$\Delta G^{\ddagger}_{186}$[a]/ kJ mol^{-1}
H	57.6 ± 0.5	−7.0 ± 1.8	59.7 ± 0.7	58.9 ± 0.6	36.7
Me	57.4 ± 0.7	−8.3 ± 2.4	59.9 ± 1.0	58.9 ± 0.8[b]	38.1[b]

[a] There is no statistical error for this quantity. We assume error bars of ±2 kJ mol^{-1}. [b] $\Delta G^{\ddagger}$ is reported at 184 K for R = Me.

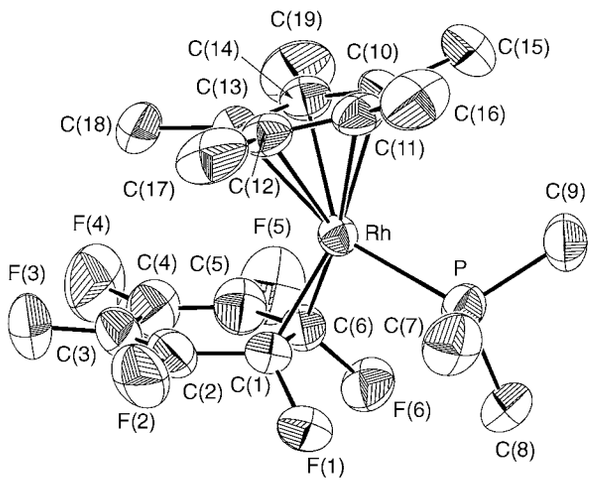

Fig. 8 An ORTEP[35] diagram (50% ellipsoids) of $[Rh(\eta^5\text{-}C_5Me_5)(PMe_3)(\eta^2\text{-}C_6F_6)]$

factor of the second-order F–F coupling effects and because of the unsuitability of EXSY for faster exchange processes.

The broadening of the ^{19}F resonances for $[Re(\eta^5\text{-}C_5H_5)(CO)_2(\eta^2\text{-}C_6F_6)]$ and $[Re(\eta^5\text{-}C_5H_4Me)(CO)_2(\eta^2\text{-}C_6F_6)]$ noted on cooling below 250 K is consistent with the onset of coalescence due to the internal rotation of the η^2-co-ordinated C_6F_6. The two resonances seen around δ −151 in the spectra of $[Re(\eta^5\text{-}C_5H_5)(CO)_2(\eta^2\text{-}C_6F_6)]$ at 178.5 K and of $[Re(\eta^5\text{-}C_5H_4Me)(CO)_2(\eta^2\text{-}C_6F_6)]$ at 173 K correspond to the resonances for the fluorines attached to the η^2-co-ordinated carbons for the two rotamers. The remaining ^{19}F resonances must have smaller chemical shift differences for the rotamers as expected for nuclei distant from the point of co-ordination.

For $[Re(\eta^5\text{-}C_5H_5)(CO)_2(\eta^2\text{-}C_6F_6)]$ in $[^2H_8]$thf the coalescence point is reached at 186 K for the δ −151 resonance. Using the separation between the resonances around δ −151 measured at 178.5 K as the separation at slow exchange, the rate constant for interconversion of the rotamers at 186 K, k_{rot}, is 53.1 s^{-1} and the free energy of activation, $\Delta G^{\ddagger}_{186}$, is 36.7 kJ mol^{-1}. For comparison, $\Delta G^{\ddagger}_{186}$ for the 'ring-whizzing' process at 186 K is calculated to be 58.9 ± 0.6 kJ mol^{-1}.

For $[Re(\eta^5\text{-}C_5H_4Me)(CO)_2(\eta^2\text{-}C_6F_6)]$ in $[^2H_8]$thf the coalescence point is reached at the slightly lower temperature of 184 K for the δ −152 resonance. The rate constant at 184 K, k_{rot}, is 59.3 s^{-1} and the free energy of activation, $\Delta G^{\ddagger}_{184}$, is 38.1 kJ mol^{-1}. For comparison, $\Delta G^{\ddagger}_{184}$ for the 'ring-whizzing' process at 184 K is calculated to be 58.9 ± 0.8 kJ mol^{-1}.

Crystal and molecular structure of $[Rh(\eta^5\text{-}C_5Me_5)(PMe_3)(\eta^2\text{-}C_6F_6)]$

The complex $[RhH(\eta^5\text{-}C_5Me_5)(PMe_3)(C_6H_5)]$ has been shown to be a good thermal source of $[Rh(\eta^5\text{-}C_5Me_5)(PMe_3)]$.[24] Accordingly, a sample of $[RhH(\eta^5\text{-}C_5Me_5)(PMe_3)(C_6H_5)]$ was heated in C_6F_6 (80 °C for 27 h) resulting in elimination of benzene and the formation of $[Rh(\eta^5\text{-}C_5Me_5)(PMe_3)(\eta^2\text{-}C_6F_6)]$.

Table 5 Bond lengths (Å) and angles (°) for $[Rh(\eta^5\text{-}C_5Me_5)(PMe_3)(\eta^2\text{-}C_6F_6)]$ with e.s.d.s in the least significant figure(s) in parentheses

Rh–C(6)	2.050(5)	C(1)–C(2)	1.460(7)
Rh–C(1)	2.059(5)	C(1)–C(6)	1.459(7)
Rh–C(13)	2.255(5)	C(2)–C(3)	1.317(8)
Rh–C(11)	2.260(4)	C(3)–C(4)	1.426(9)
Rh–C(12)	2.278(4)	C(4)–C(5)	1.329(8)
Rh–C(10)	2.285(5)	C(5)–C(6)	1.437(7)
Rh–C(14)	2.288(5)	C(10)–C(14)	1.385(7)
Rh–P	2.299(2)	C(10)–C(11)	1.454(7)
P–C(9)	1.821(5)	C(10)–C(15)	1.513(7)
P–C(8)	1.820(5)	C(11)–C(12)	1.415(7)
P–C(7)	1.821(6)	C(11)–C(16)	1.503(7)
F(1)–C(1)	1.403(5)	C(12)–C(13)	1.423(7)
F(2)–C(2)	1.351(6)	C(12)–C(17)	1.492(7)
F(3)–C(3)	1.354(7)	C(13)–C(14)	1.420(7)
F(4)–C(4)	1.353(7)	C(13)–C(18)	1.506(7)
F(5)–C(5)	1.353(6)	C(14)–C(19)	1.526(7)
F(6)–C(6)	1.401(5)		
C(6)–Rh–C(1)	41.6(2)	C(2)–C(3)–C(4)	120.8(6)
C(6)–Rh–C(13)	108.2(2)	F(3)–C(3)–C(4)	117.1(6)
C(1)–Rh–C(13)	105.7(2)	C(5)–C(4)–F(4)	121.6(7)
C(6)–Rh–C(11)	168.0(2)	C(5)–C(4)–C(3)	120.7(6)
C(1)–Rh–C(11)	142.4(2)	F(4)–C(4)–C(3)	117.5(6)
C(13)–Rh–C(11)	60.8(2)	C(4)–C(5)–F(5)	120.5(6)
C(6)–Rh–C(12)	137.0(2)	C(4)–C(5)–C(6)	122.4(6)
C(1)–Rh–C(12)	111.2(2)	F(5)–C(5)–C(6)	117.1(5)
C(13)–Rh–C(12)	36.6(2)	F(6)–C(6)–C(5)	109.3(4)
C(11)–Rh–C(12)	36.3(2)	F(6)–C(6)–C(1)	115.9(4)
C(6)–Rh–C(10)	134.7(2)	C(5)–C(6)–C(1)	117.1(5)
C(1)–Rh–C(10)	165.3(2)	F(6)–C(6)–Rh	120.0(3)
C(13)–Rh–C(10)	60.3(2)	C(5)–C(6)–Rh	120.2(4)
C(11)–Rh–C(10)	37.3(2)	C(1)–C(6)–Rh	69.5(3)
C(12)–Rh–C(10)	61.0(2)	C(14)–C(10)–C(11)	107.7(4)
C(6)–Rh–C(14)	108.0(2)	C(14)–C(10)–C(15)	125.2(5)
C(1)–Rh–C(14)	130.6(2)	C(11)–C(10)–C(15)	126.4(5)
C(13)–Rh–C(14)	36.4(2)	C(14)–C(10)–Rh	72.5(3)
C(11)–Rh–C(14)	60.5(2)	C(11)–C(10)–Rh	70.4(3)
C(12)–Rh–C(14)	60.6(2)	C(15)–C(10)–Rh	129.5(4)
C(10)–Rh–C(14)	35.2(2)	C(12)–C(11)–C(10)	107.7(4)
C(6)–Rh–P	95.6(2)	C(12)–C(11)–C(16)	124.8(5)
C(1)–Rh–P	91.6(2)	C(10)–C(11)–C(16)	126.1(5)
C(13)–Rh–P	156.24(13)	C(12)–C(11)–Rh	72.5(3)
C(11)–Rh–P	95.53(13)	C(10)–C(11)–Rh	72.3(3)
C(12)–Rh–P	121.91(14)	C(16)–C(11)–Rh	131.2(4)
C(10)–Rh–P	103.10(14)	C(11)–C(12)–C(13)	107.4(4)
C(14)–Rh–P	135.85(14)	C(11)–C(12)–C(17)	126.7(5)
C(9)–P–C(8)	99.2(3)	C(13)–C(12)–C(17)	125.9(5)
C(9)–P–C(7)	102.7(3)	C(11)–C(12)–Rh	71.1(3)
C(8)–P–C(7)	101.5(3)	C(13)–C(12)–Rh	70.8(3)
C(9)–P–Rh	116.7(2)	C(17)–C(12)–Rh	125.7(3)
C(8)–P–Rh	123.2(2)	C(14)–C(13)–C(12)	108.4(4)
C(7)–P–Rh	110.7(2)	C(14)–C(13)–C(18)	124.7(5)
F(1)–C(1)–C(2)	110.0(4)	C(12)–C(13)–C(18)	125.4(5)
F(1)–C(1)–C(6)	116.3(4)	C(14)–C(13)–Rh	73.1(3)
C(2)–C(1)–C(6)	117.1(5)	C(12)–C(13)–Rh	72.6(3)
F(1)–C(1)–Rh	118.9(3)	C(18)–C(13)–Rh	131.6(4)
C(2)–C(1)–Rh	120.5(4)	C(10)–C(14)–C(13)	108.8(4)
C(6)–C(1)–Rh	68.9(3)	C(10)–C(14)–C(19)	125.6(5)
C(3)–C(2)–F(2)	121.5(6)	C(13)–C(14)–C(19)	125.4(5)
C(3)–C(2)–C(1)	121.9(6)	C(10)–C(14)–Rh	72.3(3)
F(2)–C(2)–C(1)	116.6(6)	C(13)–C(14)–Rh	70.5(3)
C(2)–C(3)–F(3)	122.0(7)	C(19)–C(14)–Rh	127.0(4)

The complex has already been fully characterised by multinuclear NMR and IR spectroscopy.[24] Unlike the Re case, this complex is stereochemically rigid and exhibits one isomer over the wide temperature range explored. Small orange crystals were grown from diethyl ether solution at room temperature and X-ray crystallography confirmed their identity as [Rh(η^5-C_5Me_5)(PMe_3)(η^2-C_6F_6)].

The crystal structure of [Rh(η^5-C_5Me_5)(PMe_3)(η^2-C_6F_6)] proved free of the disorder problems which limited the reliability of the structure of the C_5H_5 analogue. This is the first structure of an η^2-C_6F_6 complex of a second-row metal which is free of disorder and provides more accurate geometric data than the structures of the Re and Ir complexes. The basic characteristics of the co-ordination geometry resemble those for the other complexes (Fig. 8, Table 5). The co-ordinated C–C bond is extended to 1.459(7) Å relative to free C_6F_6 [1.394(7) Å]. The unco-ordinated C–C bonds form a diene pattern [1.449(7) Å for mean of C(1)–C(2) and C(6)–C(5), 1.323(8) Å for mean of C(2)–C(3) and C(4)–C(5) and 1.426(9) Å for C(3)–C(4)]. The C–F bonds for C(1) and C(6) average 1.402(5) Å compared to 1.353(6) Å for the remainder, an extension of 0.049 Å or approximately 10 e.s.d.s. The Rh atom lies 1.920(5) Å from the midpoint of C(1)–C(6) [labelled D(2)]. The distance from the Rh to the centroid of C_5Me_5 [D(1)] is 1.926(5) Å and the D(1)–Rh–D(2) angle is 140.1°. There is a short contact between F(6) and one of the PMe_3 carbon atoms, C(8), of 2.805 Å accounting for the significant coupling J_{FH} observed in the ^{1}H NMR spectrum.

Discussion

The photoreaction of [Re(η^5-C_5Me_5)($CO)_3$] with C_6F_6 yields the HF elimination product [Re(η^6-$C_5Me_4CH_2$)$(CO)_2(C_6F_5)$].[31] In contrast, [Re(η^5-C_5H_5)$(CO)_3$] and [Re(η^5-C_5H_4Me)$(CO)_3$] react to form simple η^2-C_6F_6 complexes.

Comparison of crystal structures

The structural parameters of the four [M](η^2-C_6F_6) complexes investigated crystallographically are shown in Table 6. The principal features are shown diagrammatically in Fig. 9 as mean bond angles and distances, with the figures in parentheses showing the range for three of the complexes, rather than the e.s.d.s. The data for [M] = Rh(η^5-C_5H_5)(PMe_3) may be taken to be less accurate than the remainder because of disorder in the PMe_3 group, and are omitted from Fig. 9. The co-ordinated C–C bond averages 1.47 Å and varies in length by ±0.01 Å. The geometry of the unco-ordinated diene unit varies even less. The angle between the C_6F_4 plane and the C(1)C(6)F(1)F(6) plane averages 45.9° and varies by ±1.3°. The angle between the C_6F_4 plane and the MC(1)C(6) plane averages 114.3° and varies by ±0.4°. Thus it can be seen that the C_6F_6 ligand resembles a co-ordinated alkene in geometry. The analogy may be pursued by examining the distortion of the hexafluorobenzene by Ibers' method[43] for a co-ordinated alkene. The angles α, β, γ and δ (Fig. 10) are close to those for the C_2F_4 unit of C_2F_4 complexes.[44,45] Pörschke *et al.*[46] have recently determined the crystal structure of another η^2-C_6F_6 complex, [Ni(dbpe)(η^2-C_6F_6)-(dbpe $Bu^t_2PCH_2CH_2PBu^t_2$)]. The structural features of the

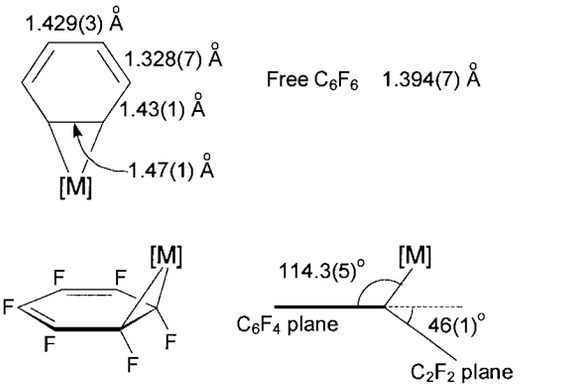

Fig. 9 Principal structural features of [M](η^2-C_6F_6) complexes: mean of data from [M] = Re(η^5-C_5H_5)$(CO)_2$, Rh(η^5-C_5Me_5)(PMe_3) and Ir(η^5-C_5H_5)(C_2H_4). The figures in brackets represent the range of values of bond lengths or angles measured for the three complexes. In the exceptional case of free C_6F_6 the figure represents the e.s.d. for the bond length

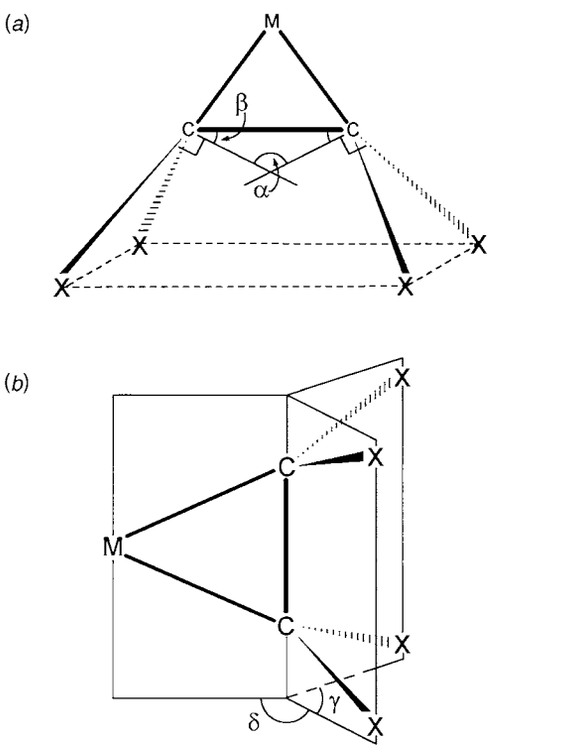

Fig. 10 Diagram of co-ordinated alkene M(η^2-C_2X_4) defining the angles of deformation following Ibers. (*a*) The angle α is defined as the angle between the normals to the CX_2 planes. The angle β is the angle between one of these normals and the C–C vector. (*b*) The angle γ is the torsional angle X–C–C–X′ where X and X′ are *trans* to one another. The angle δ is the torsional angle M–C–C–X. As bending back of the alkene increases, α increases from 0°, β decreases from 90°, γ decreases from 180° and δ increases from 90°

Table 6 Structural parameters for [M](η^2-C_6F_6)

[M]	C(1)–C(6)/Å	Mean of C(1)–C(2) and C(6)–C(5)/Å	Mean of C(2)–C(3) and C(4)–C(5)/Å	C(3)–C(4)/Å	Angle between planes C_6F_4 and C(1)C(6)F(1)F(6)/°	Angle between planes C_6F_4 and MC(1)C(6)/°
Rh(C_5Me_5)(PMe_3)	1.459(7)	1.449(7)	1.323(8)	1.426(9)	46.4(2)	114.3(3)
Re(C_5H_5)$(CO)_2$	1.476(12)	1.430(12)	1.325(12)	1.430(13)	44.4(2)	113.8(3)
Ir(C_5H_5)(C_2H_4)[25]	1.47(2)	1.425(20)	1.335(20)	1.43(2)	47.0	114.6
Rh(C_5H_5)(PMe_3)[24]	1.397(12)	1.473(8)	1.331(8)	1.354(12)	43.8	108.6

Table 7 Distortions of the hexafluorobenzene moiety in $[M](\eta^2\text{-}C_6F_6)$ and $[M](\eta^2\text{-}C_2F_4)$ analysed by Ibers' method

$[M](\eta^2\text{-}C_6F_6)$	D(2)–M	α/°	β/°	|γ|/°	|δ|/°
$Rh(C_5Me_5)(PMe_3)$	1.920(5)	78.1(6)	51.0	132.9, 131.3	114.4, 112.8
$Re(C_5H_5)(CO)_2$	2.059(7)	76.2(8)	51.9	130.8, 138.0	108.7, 114.1
$Ir(C_5H_5)(C_2H_4)$[25]	1.941(2)	76.7	51.8	132.5	113.5
$[M](\eta^2\text{-}C_2F_4)$					
$Rh(C_5H_5)(C_2H_4)$[44]	1.898(5)	74.3	52.8	131.4	114.3
$Ru(C_5Me_5)(acac)$[45]	1.925(6)	73.9	53.0	131.0	114.5
$[(C_5Me_5)Ru(C_2F_4)Cl]_2$[45]	1.929(5)	73.7	53.1	131.0	114.5

* D(2) is defined as the centre of the co-ordinated C–C bond of C_6F_6 or C_2F_4.

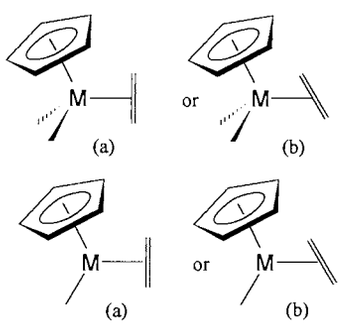

co-ordinated C_6F_6 resemble those of the four $[M](\eta^2\text{-}C_6F_6)$ complexes investigated previously, with a co-ordinated C–C bond of 1.486(6) Å, an angle between the C_6F_4 plane and the C(1)C(6)F(1)F(6) plane of 44° and an angle between the C_6F_4 plane and the MC(1)C(6) plane of 114°.

Although there is minimal difference between the geometries of the C_6F_6 ligand in the three disorder-free structures reported here, there is a notable difference in the distance between ligand and metal [M–D(2)]. The Re–D(2) distance in $[Re(\eta^5\text{-}C_5H_5)(CO)_2(\eta^2\text{-}C_6F_6)]$ is 0.12 Å longer than the Ir–D(2) distance in $[Ir(\eta^5\text{-}C_5H_5)(C_2H_4)(\eta^2\text{-}C_6F_6)]$.[25] This extension may well contribute to the lower barrier to ring rotation and ring whizzing in the rhenium complex by reducing steric effects.

Theoretical work has been reported on the preferred orientation of alkenes co-ordinated to the fragments $M(\eta^5\text{-}C_5H_5)L_2$ (isolobal to ML_5) and $M(\eta^5\text{-}C_5H_5)L$ (isolobal to ML_4).[47–50] In each case, conformation (b) is preferred, as observed in the crystal structures of the complexes reported here.[47–50]

Ligand effect of $\eta^2\text{-}C_6F_6$

In 1979, Timney[51] proposed a method for predicting $\tilde{\nu}$(CO) values for mononuclear transition-metal carbonyls. Using energy factoring, the stretching force constants, k_{CO}, were evaluated using the relationship (5) where k_d is the stretching

$$k_{CO} = k_d + \sum_L \varepsilon_L{}^\theta \qquad (5)$$

force constant for an isolated M(CO) unit with the appropriate number of d electrons and $\varepsilon_L{}^\theta$ are 'ligand effect constants', which quantify the effect of adding a ligand, L, at an angle θ to the M(CO) unit. Thus, the $\tilde{\nu}$(CO) values for a series of $[Re(\eta^5\text{-}C_5H_5)(CO)_2L]$ complexes can be used to determine a 'ligand effect constant' for C_6F_6 and to assess the electronic characteristics of C_6F_6 as a ligand (Table 8). The $\tilde{\nu}$(CO) frequencies of $[Re(\eta^5\text{-}C_5H_5)(CO)_2(\eta^2\text{-}C_6F_6)]$ are higher than those of any other $[Re^I(\eta^5\text{-}C_5H_5)(CO)_2L]$ complex. The values for one of the rotamers are close to those for $[Re^{III}(H)_2(\eta^5\text{-}C_5H_5)(CO)_2]$ (Table 9). If the bonding in η^2-co-ordinated C_6F_6 is viewed in terms of the Dewar–Chatt model for alkene bonding[47,49,57] the system can be considered as approaching the metallacyclopropane extreme (left) where the alkene acts as a strong acceptor ligand,

Table 8 Ligand effect constants, experimental and calculated $\tilde{\nu}$(CO) frequencies for $[Re(C_5H_5)(CO)_2L]$

L	Ligand effect constant, ε_L	$\tilde{\nu}$/cm^{-1}	
		Experimental[a]	Calculated
PMe_3[b]	−38.7[f]	1937, 1872	1950, 1876
C_2H_4[c]	4.0[f]	1978, 1911	1974, 1906
PPh_3[b]	−31.7[f]	1943, 1881	1954, 1881
N_2[d]	6.0[f]	1974, 1920	1976, 1908
CO	37.3[f]	2031, 1940	2024, 1930
$\eta^2\text{-}C_6F_6$ (i)[e]	98.9	2030, 1970	—
$\eta^2\text{-}C_6F_6$ (ii)[e]	82.0	2022, 1957	—

[a] All IR data in hexane, except PPh_3 in cyclohexane. [b] Ref. 52. [c] Ref. 53. [d] Ref. 54. [e] (i) and (ii) denote the two rotamers. [f] Ref. 51.

Table 9 Infrared stretching frequences, $\tilde{\nu}$(CO), of $[ReX_2(CO)_2(C_5H_5)]$ complexes

Complex	$\tilde{\nu}$/cm^{-1}
cis-$[ReCl_2(CO)_2(C_5H_5)]$[a]	2061, 1988[c]
cis-$[ReI_2(CO)_2(C_5H_5)]$[a]	2040, 1977[d]
trans-$[ReH_2(CO)_2(C_5H_5)]$[b]	2022, 1954[d]

[a] Ref. 55. [b] Ref. 56. [c] In $CHCl_3$. [d] In alkane.

as contrasted with the extreme of minimal π back donation (right). Thus the electron-withdrawing character of $\eta^2\text{-}C_6F_6$ is indicated both by the IR data and by the similarity of the structures of complexes with co-ordinated C_2F_4 and C_6F_6.

The $\tilde{\nu}$(CO) frequencies of $[Re(\eta^5\text{-}C_5H_5)(CO)_2L]$ provide a continuous scale of electron density at the metal, which is not accessible for the compounds without carbonyl ligands. On the other hand, the Rh–P coupling constants of $Rh(\eta^5\text{-}C_5R_5)(PMe_3)$ complexes have proved characteristic of the oxidation state of the metal, with values close to 150 Hz for many rhodium(III) complexes and 200 Hz for rhodium(I) complexes.[1] This parameter points unequivocally to an Rh^I formulation for $[Rh(\eta^5\text{-}C_5R_5)(PMe_3)(\eta^2\text{-}C_6F_6)]$ (R = H or Me).[24]

Fluxional behaviour

For $[Re(\eta^5\text{-}C_5H_4R)(CO)_2(\eta^2\text{-}C_6F_6)]$ (R = Me or H) the rapid ring-rotation process that interconverts the two rotamers is analogous to the propeller rotation observed in many alkene complexes.[47] High barriers to propeller rotation are generally found in complexes with electronegative substituents on the alkene.[45] Since such complexes show metallacyclopropane structures, it is easy to suppose that a metallacyclopropane structure will lead to a high barrier for rotation.[45] An example is

Table 10 Crystallographic parameters for [Re(η^5-C_5H_5)(CO)$_2$(η^2-C_6F_6)] and [Rh(η^5-C_5Me_5)(PMe_3)(η^2-C_6F_6)]

	[Re(η^5-C_5H_5)(CO)$_2$(η^2-C_6F_6)]	[Rh(η^5-C_5Me_5)(PMe_3)(η^2-C_6F_6)]
Empirical formula	$C_{13}H_5F_6O_2Re$	$C_{19}H_{24}F_6PRh$
M	493.37	500.26
Colour, dimensions/mm	Pink, 0.40 × 0.25 × 0.10	Orange, 0.30 × 0.10 × 0.10
a/Å	7.926(2)	8.694(9)
b/Å	12.179(4)	16.818(9)
c/Å	13.675(4)	14.642(6)
β/°	102.91(2)	106.69(6)
U/Å^3	1286.6(6)	2051(3)
D_c/g cm^{-3}	2.547	1.620
F(000)	912	1008
μ(Mo-Kα)/cm^{-1}	95.22	9.64
hkl Index ranges	0–9, 0–14, −16 to 15	0–9, 0–20, −17 to 16
θ Range/°	2.27–25	2.73–25
No. reflections measured, unique	2273, 2272 (R_{int} = 0)	4019, 3618 (R_{int} = 0.040)
No. of variables	200	253
Reflection/parameter ratio	11.4	14.3
Residuals [$I > 2\sigma(I)$]	$R1$ = 0.0258, $wR2$ = 0.0851	$R1$ = 0.0349, $wR2$ = 0.0725
Residuals (all data)	$R1$ = 0.0380, $wR2$ = 0.0971	$R1$ = 0.0731, $wR2$ = 0.0859
Goodness of fit on F^2	0.770	0.995
a, *b* In weighting scheme, *w*	0.10, 0	0.0348, 1.1158
Largest difference peak, hole/e Å^{-3}	0.718, −0.685	0.339, −0.438

Details in common: monoclinic, space group $P2_1/n$, $Z = 4$, Rigaku AFC6S diffractometer, Mo-Kα radiation (λ = 0.710 69 Å), T = 293(2) K, refined by full-matrix least squares on F^2. $w^{-1} = \sigma^2(F_o)^2 + (aP)^2 + bP$ where $P = (F_o^2 + 2F_c^2)/3$.

d^8 [Rh(η^5-C_5H_5)(C_2F_4)(C_2H_4)] where rapid rotation of the C_2H_4 ligand is observed, while rotation of the co-ordinated C_2F_4 is not detectable up to 100 °C.[44] Curnow *et al.*[45] have recently reported that facile propeller rotation ($\Delta G^\ddagger = 55 \pm 2$ kJ mol^{-1}) is also observed in the d^6 metallacyclopropane complex [Ru(η^5-C_5Me_5)(acac)(η^2-C_2F_4)] (acac = acetylacetonate). The two types of complex under study here have very similar co-ordination geometries for C_6F_6, but quite different barriers to rotation. For [Re(η^5-C_5H_4R)(CO)$_2$(η^2-C_6F_6)] (R = H or Me) the barrier is *ca.* 37 kJ mol^{-1}, for [Rh(η^5-C_5Me_5)(PMe_3)(η^2-C_6F_6)] the barrier to rotation is too high to measure.

From theoretical studies, it is proposed that low rotation barriers should be found in complexes where the alkene is bound to a d^6 ML_5 fragment or an isolobal analogue.[49,58] In d^6 ML_5 fragments there are two filled, orthogonal and degenerate metal d orbitals available for π back bonding to the alkene, so the back bonding interaction is cylindrically symmetric.[49] Since the Re(η^5-C_5H_4R)(CO)$_2$ and Ru(η^5-C_5Me_5)(acac) fragments are isolobal with d^6 ML_5 fragments, the low rotation barriers observed both for [Re(η^5-C_5H_4R)(CO)$_2$(η^2-C_6F_6)] (R = H or Me) and [Ru(η^5-C_5Me_5)(acac)(η^2-C_2F_4)] can be explained.[45,50,58] Another example of an analogue of d^6 ML_5 with a low barrier is [Fe(η^5-C_5H_5)(CO)$_2$(C_2H_4)]$^+$ ($\Delta G^\ddagger$ = 32.6 kJ mol^{-1}).[59]

Curnow *et al.*[45] state clearly that there should be no correlation between acceptor properties of an alkene and the barrier to propeller rotation. They note that differences in the barrier arise from variations in the symmetries and energies of the frontier orbitals presented by the metal fragment to the alkene, differences in orbital overlap along the rotation path and other attractive or repulsive interactions in the transition state. Studies of [Ru(η^5-C_5H_5)(L_2)(alkene)]$^+$ (L = PPh_3, L_2 = 1,4-diisopropyl-1,4-diazabuta-1,3-diene or 1,4-di-*p*-tolyl-1,4-diazabuta-1,3-diene) complexes have confirmed that the barrier to rotation of the alkene does not correlate with the strength of the metal–alkene interaction in the ground state.[60] In contrast, quantum calculations[61] predict that the barrier to rotation in [Pt(PH_3)$_2$(C_2H_4)] will be higher when the alkene is constrained to be highly pyramidalised than in the unconstrained case. Such pyramidalisation is associated with stronger bonding. In the absence of electronic effects, the rotation barrier must arise from some unfavourable steric interaction in the transition state. The long Re–C_6F_6 distance [Re–D(2)] in [Re(η^5-C_5H_5)(CO)$_2$(η^2-C_6F_6)] will serve to reduce steric effects and keep the barrier low.

Until the recent paper of Pörschke *et al.*,[46] the ring-whizzing process noted for [Re(η^5-C_5H_4R)(CO)$_2$(η^2-C_6F_6)] (R = Me or H) had not been observed in η^2-C_6F_6 complexes. In his investigation of the rearrangement of metals on π-systems, Mann[39] states that in all η^n-C_mH_m ($n < m$) ring systems (with the exception of η^6-C_8H_8), whizzing proceeds by a [1,2]-shift as observed here. Mann related the variations in barriers to the Woodward–Hoffmann rules.[39,62] All η^2-C_6F_6 complexes have proved stereochemically rigid except for the rhenium complexes reported here and the d^{10} 16 e$^-$ [Ni(dbpe)(η^2-C_6F_6)] which shows equivalent fluorine nuclei down to 193 K.[46] Pörschke *et al.* propose an 18 e$^-$ η^4-C_6F_6 complex as an intermediate in the ring-whizzing. The related 16 e$^-$ nickel(0) complexes [Ni{η^2-$C_6(CF_3)_6$}L_2] [L_2 = C_8H_{12}, L = P(OR)$_3$ or PR_3],[63] are also fluxional at low temperature, but a barrier of *ca.* 45 kJ mol^{-1} was reported for the platinum analogue, [Pt{η^2-$C_6(CF_3)_6$}(PEt_3)$_2$].[63] Although NMR spectra of η^2-C_6H_6 complexes are commonly reported to show averaging of the benzene resonances, we have found no quantitative investigations.[4–7,64]

In 1984, Jones and Feher[1a] proposed a mechanism for the isomerisation of [RhH(η^5-C_5Me_5)(PMe_3)(C_6D_5)] involving the intermediacy of an η^2-arene species. The isomerisation was found to proceed stepwise around the ring, indicating that ring-whizzing in the η^2-arene intermediate is slow compared to oxidative addition. This contrasts with the rapid ring-whizzing detected for [Re(η^5-C_5H_4R)(CO)$_2$(η^2-C_6F_6)] (R = Me or H).

Conclusion

(1) The photochemical reactions of [Re(η^5-C_5H_4R)(CO)$_3$] with C_6F_6 yield [Re(η^5-C_5H_4R)(CO)$_2$(η^2-C_6F_6)] (R = H or Me). (2) The IR spectra of these complexes reveal the presence of two rotamers. (3) The variable-temperature ^{19}F NMR spectra demonstrate that interconversion of the rotamers is very rapid ($\Delta G^\ddagger \approx 37$ kJ mol^{-1} at 186 K). The complexes also undergo fast ring-whizzing *via* intramolecular [1,2]-shift processes with $\Delta H^\ddagger \approx 57$ kJ mol^{-1} and $\Delta S^\ddagger \approx -8$ J K^{-1} mol^{-1}. (4) The crystal structure of [Re(η^5-C_5H_5)(CO)$_2$(η^2-C_6F_6)] reveals distortion of the C_6F_6 moiety to form a co-ordinated alkene and an

unco-ordinated diene unit. The same features are observed in the structure of $[Rh(\eta^5\text{-}C_5Me_5)(PMe_3)(\eta^2\text{-}C_6F_6)]$. The metal–carbon ($C_6F_6$) bonds of the rhenium complex are considerably longer than those of the rhodium complex. (5) The geometry of the C_6F_6 ligand in three $M(\eta^2\text{-}C_6F_6)$ complexes is shown to vary minimally pointing to high force constants for alteration of this structure. It is close to the metallacyclopropane limit. (6) The CO stretching frequencies of $[Re(\eta^5\text{-}C_5H_4R)(CO)_2(\eta^2\text{-}C_6F_6)]$ are indicative of electron density at the metal closer to that in rhenium(III) than in rhenium(I) complexes. However, the fluxional behaviour of the rhenium complexes and the values of J(Rh–P) in the rhodium complexes support a metal–alkene formulation for $\eta^2\text{-}C_6F_6$ complexes. (7) The low barrier to rotation about the metal–C_6F_6 bond is associated with the electronic structure of the $Re(\eta^5\text{-}C_5H_5)(CO)_2$ unit, isolobal with d^6 ML_5, and the longer metal–ligand bonds of the rhenium complex compared to the d^8 analogues.

Experimental

General methods

All syntheses and manipulations were performed under argon using standard Schlenk and high vacuum techniques, or in a glove box. Dirhenium decacarbonyl (98%) was purchased from Aldrich and used without further purification. All solvents for general use were dried by refluxing over sodium–benzophenone and distilled under argon. Hexafluorobenzene (99.9%) from Aldrich was condensed onto molecular sieves (grade 4 Å) under vacuum prior to use. Deuteriated solvents were obtained from Goss and dried over potassium and vacuum distilled before use. The solutions, prepared in small Pyrex ampoules fitted with PTFE taps, were degassed with three freeze–pump–thaw cycles and then back-filled with argon before irradiation with either an Applied Photophysics 250 W high-pressure mercury arc with a water filter to remove excess heat or a Rayonet RPR-100 photochemical reactor. Reaction mixtures requiring irradiation through a thin film were placed in a Pyrex sleeve reactor (path-length 2 mm, volume 15 cm^3) with Schlenk connections. The sleeve reactor fitted over the Pyrex immersion-well of an Applied Photophysics reactor (RB125) with an immersible 125 W medium-pressure mercury lamp. All NMR tubes (Wilmad 528-PP) were either fitted with Young's taps to allow sealing under an argon atmosphere, or were flame sealed under vacuum.

Spectroscopic methods

Infrared spectra were recorded on a Mattson Unicam Research Series FTIR spectrometer, linked to a PC with 'WINFIRST' software. The sample chamber was purged with dry, CO_2-free air. Low-temperature IR measurements were carried out using a vacuum-tight liquid cell with CaF_2 windows (cooled with dry ice–acetone slush) supplied by Graseby Specac. Most one- and all two-dimensional NMR spectra were recorded on a Bruker AMX500 spectrometer. Additionally some spectra were recorded using a Bruker MSL300 and a JEOL FX 90Q. Proton NMR chemical shifts were referenced to residual protiated solvent: $[^2H_8]$thf (δ 1.80), $^{13}C\text{-}\{^1H\}$ NMR chemical shifts were referenced to solvent peaks: $[^2H_8]$thf (δ 26.7), ^{19}F NMR spectra are referenced to external $CFCl_3$ at δ 0.0 or to internal C_6F_6 at δ −162.9 and $^{31}P\text{-}\{^1H\}$ NMR chemical shifts were referenced to external H_3PO_4 (85%) at δ 0.0. The temperatures for variable-temperature NMR spectroscopy were calibrated using a sample of 100% methanol in a capillary inside the NMR tubes.[65] The ^{19}F NMR spectrum of $[Re(\eta^5\text{-}C_5H_5)(CO)_2(\eta^2\text{-}C_6F_6)]$ belongs to an $[AMX]_2$ spin system[66] which was simulated using the WINDAISY 2.1 (Bruker-Franzen Analytik GmbH) and gNMR version 3.6 (Cherwell Scientific) packages. Mass spectra were recorded on a VG Autospec.

Matrix isolation

The matrix isolation equipment has been described previously.[67] Samples were deposited onto a CsI window cooled by an Air Products CS202 closed-cycle Displex refrigerator to 20 K. The compound $[Re(\eta^5\text{-}C_5H_5)(CO)_2(\eta^2\text{-}C_6F_6)]$ was sublimed from a right-angled glass tube (at 323 K) at the same time as matrix gas (BOC Research Grade argon, 99.999%) was deposited through a separate inlet. Typical deposition rates were 2 mmol h^{-1} for Ar. The samples were cooled to 12 K before recording IR spectra, 1 cm^{-1} resolution, 128 scans coaveraged.

Crystallographic methods

Crystals of $[Re(\eta^5\text{-}C_5H_5)(CO)_2(\eta^2\text{-}C_6F_6)]$ suitable for X-ray diffraction were obtained by recrystallisation from hexane at 253 K. Small orange crystals of $[Rh(\eta^5\text{-}C_5Me_5)(PMe_3)(\eta^2\text{-}C_6F_6)]$ suitable for X-ray diffraction were grown from diethyl ether solution at room temperature. The crystallographic parameters for the two complexes are summarised in Table 10. In each case a single crystal was mounted on a glass fibre in epoxy cement. Data were collected on a Rigaku AFC6S diffractometer. Data reduction, application of Lorentz, polarisation and 2θ-dependent absorption corrections were applied with the TEXSAN system.[68] The structure was solved by direct methods with full-matrix least-squares refinement carried out using the TEXSAN software package.[68] The hydrogen atoms were included at calculated sites and refined with a 'riding' model. Final refinement was carried out using SHELXL 93.[69]

Atomic coordinates, thermal parameters, and bond lengths and angles have been deposited at the Cambridge Crystallographic Data Centre (CCDC). See Instructions for Authors, *J. Chem. Soc., Dalton Trans.*, 1997, Issue 1. Any request to the CCDC for this material should quote the full literature citation and the reference number 186/441.

Syntheses

The syntheses of $[Rh(\eta^5\text{-}C_5Me_5)(PMe_3)(\eta^2\text{-}C_6F_6)]$[24] and $[Re(\eta^5\text{-}C_5H_5)(CO)_3]$[70] have been reported previously. The compound $[Re(\eta^5\text{-}C_5H_4Me)(CO)_3]$ was prepared using an analogous procedure to that of Casey *et al.*[70b] for $[Re(\eta^5\text{-}C_5H_5)(CO)_3]$: $[Re(CO)_5Br]$ and sodium methylcyclopentadienyl (5% excess) were refluxed in benzene for 4 h, $[Re(\eta^5\text{-}C_5H_4Me)(CO)_3]$ was isolated by extraction with hexane followed by column chromatography over alumina to remove traces of $[Re_2(CO)_{10}]$ (63% yield).

$[Re(\eta^5\text{-}C_5H_5)(CO)_2(\eta^2\text{-}C_6F_6)]$. The compound $[Re(\eta^5\text{-}C_5H_5)(CO)_3]$ (90–100 mg) was dissolved in hexafluorobenzene (≈8 cm^3) in a sleeve reactor. The sleeve reactor was fitted over the immersion-well of an Applied Photophysics reactor and the mixture photolysed for 8 h. The excess hexafluorobenzene was removed under vacuum and the oily brown residue was successively extracted with 7 cm^3 portions of hexane. The IR spectrum in hexane solution showed absorptions at 2030 and 1940 cm^{-1} for $[Re(\eta^5\text{-}C_5H_5)(CO)_3]$ and 2030, 2022, 1970 and 1957 cm^{-1} for $[Re(\eta^5\text{-}C_5H_5)(CO)_2(\eta^2\text{-}C_6F_6)]$ in the ratio ≈5:1. The solution was reduced in volume, at room temperature, to ≈10 cm^3. The resulting precipitate was separated from the solution {which contained unreacted $[Re(\eta^5\text{-}C_5H_5)(CO)_3]$}, washed twice with ≈2 cm^3 of cold hexane and dried under vacuum to yield $[Re(\eta^5\text{-}C_5H_5)(CO)_2(\eta^2\text{-}C_6F_6)]$. The product was recrystallised twice from hexane–diethyl ether (16:1) at −20 °C to give a pale pink solid in low yield (*ca.* 10%) (Found: C, 31.55; H, 1.05. Calc. for $C_{13}H_5F_6O_2Re$: C, 31.60; H, 1.00%). NMR ($[^2H_8]$thf, 300 K): ^1H, δ 5.53 (s, C_5H_5); $^{13}C\text{-}\{^1H\}$, δ 92.2 (s, C_5H_5), 197.5 (CO); at 260 K the CO resonance appears as a multiplet ([AA′XX′] system; $|J_{FC} + J_{FC'}| \approx 16$ Hz)[66] and three new resonances can be seen at δ 83.4 (d, 254, C_6F_6), 132.1 (d, 256, C_6F_6), 151.2 (d, 262 Hz, C_6F_6). Electron impact mass spectrum: *m/z*

494 $[M]^+$, 438 $[M - 2CO]^+$, 419 $[Re(\eta^5\text{-}C_5H_5)(C_6F_5)]^+$, 308 $[M - C_6F_6]^+$, 280 $[M - CO - C_6F_6]^+$, 252 $[Re(\eta^5\text{-}C_5H_5)]^+$, 186 $[C_6F_6]^+$.

$[Re(\eta^5\text{-}C_5H_4Me)(CO)_2(\eta^2\text{-}C_6F_6)]$. The compound $[Re(\eta^5\text{-}C_5H_4Me)(CO)_3]$ (125–175 mg) was dissolved in hexafluorobenzene (≈10 cm^3) and degassed with three freeze–pump–thaw cycles. The mixture was irradiated for 8 h ($\lambda = 300$ nm) at room temperature using a Rayonet RPR-100 photochemical reactor in Pyrex tubes (≈1 cm external diameter). The solutions turned light brown and some brown solid formed. The solvent was removed under vacuum and the oily brown residue was successively extracted with 7 cm^3 portions of hexane. The resulting yellow solution was reduced in volume to ≈10 cm^3 at room temperature. The resulting white precipitate was separated from the solution {which contains unreacted $[Re(\eta^5\text{-}C_5H_4Me)(CO)_3]$}, washed twice with ≈2 cm^3 of cold hexane and dried under vacuum to yield $[Re(\eta^5\text{-}C_5H_4Me)(CO)_2(\eta^2\text{-}C_6F_6)]$. The product was recrystallised from hexane–diethyl ether (16:1) at −20 °C. Yield = 15% (Found: C, 32.65; H, 1.4. Calc. for $C_{14}H_7F_6O_2Re$: C, 33.15; H, 1.4%). NMR ([$^2H_8$]thf, 300 K): ^{1}H, δ 2.36 (s, $C_5H_4\mathit{Me}$), 5.36 and 5.55 (dd, $C_5\mathit{H}_4Me$, $[AX]_2$ system); ^{13}C-{^{1}H} δ 14.87 (s, $C_5H_4\mathit{Me}$), 83.6 (d, 245 Hz, C_6F_6), 90.93 and 92.87 ($MeC\mathit{C}_4H_4$), 111.51 ($MeCC_4H_4$), 132.2 (d, 262 Hz, C_6F_6), 151.2 (br, C_6F_6), 198.46 (CO); at 260 K the CO resonance appears as a multiplet ([AA′XX′] system; $|J_{FC} + J_{FC}| \approx 15.2$ Hz).[66] Chemical ionization mass spectrum: *m/z* 508 $[M]^+$, 489 $[M - F]^+$, 429 $[Re(CO)_2(C_6F_6)]^+$, 322 $[M - C_6F_6]^+$, 186 $[C_6F_6]^+$.

Acknowledgements

We would like to acknowledge the support of the EPSRC and the assistance and advice of Dr. S. B. Duckett, Dr. S. J. Heyes, A. Kraus, F. R. Manby, Professor B. E. Mann, Dr. B. A. Messerle, Dr. P. D. Morran and G. Wilson. A. H. K. thanks Universidad Catolica de Valparaiso and FONDECYT-Chile for financial support (grants DGIP 125.776-96 and 1960383 respectively). B. O. acknowledges Fundacion Andes for a Doctoral fellowship.

References

1 (*a*) W. D. Jones and F. J. Feher, *J. Am. Chem. Soc.*, 1984, **106**, 1650; (*b*) J. R. Sweet and W. A. G. Graham, *Organometallics*, 1983, **2**, 135; (*c*) S. T. Belt, S. B. Duckett, M. Helliwell and R. N. Perutz, *J. Chem. Soc., Chem. Commun.*, 1989, 928.
2 R. W. Turner and E. L. Amma, *J. Am. Chem. Soc.*, 1966, **88**, 3243; E. A. Hall and E. L. Amma, *J. Am. Chem. Soc.*, 1969, **91**, 6538; I. F. Taylor, E. A. Hall and E. L. Amma, *J. Am. Chem. Soc.*, 1969, **91**, 5745; R. W. Turner and E. L. Amma, *J. Am. Chem. Soc.*, 1966, **88**, 1877; R. W. Turner and E. L. Amma, *J. Am. Chem. Soc.*, 1963, **85**, 4046; E. A. Hall and E. L. Amma, *Chem. Commun.*, 1968, 622.
3 D. J. Brauer and C. Krüger, *Inorg. Chem.*, 1977, **16**, 884.
4 W. D. Harman and H. Taube, *Inorg. Chem.*, 1987, **26**, 2917; *J. Am. Chem. Soc.*, 1988, **110**, 7906; W. D. Harman, M. Gebhard and H. Taube, *Inorg. Chem.*, 1990, **29**, 567; H. Taube, *Pure Appl. Chem.*, 1991, **63**, 651.
5 W. D. Harman and H. Taube, *J. Am. Chem. Soc.*, 1987, **109**, 1883.
6 W. D. Harman, M. Sekine and H. Taube, *J. Am. Chem. Soc.*, 1988, **110**, 5725.
7 W. D. Harman and H. Taube, *J. Am. Chem. Soc.*, 1988, **110**, 7555.
8 W. D. Jones and L. Dong, *J. Am. Chem. Soc.*, 1989, **111**, 8722.
9 R. M. Chin, L. Dong, S. B. Duckett, M. G. Partridge, W. D. Jones and R. N. Perutz, *J. Am. Chem. Soc.*, 1993, **115**, 7685; S. T. Belt, L. Dong, S. B. Duckett, W. D. Jones, M. G. Partridge and R. N. Perutz, *J. Chem. Soc., Chem. Commun.*, 1991, 266.
10 R. M. Chin, L. Dong, S. B. Duckett and W. D. Jones, *Organometallics*, 1992, **11**, 871.
11 R. L. Thompson, S. Lee, A. L. Rheingold and N. J. Cooper, *Organometallics*, 1991, **10**, 1657.
12 J. Merket, R. M. Nielson, M. J. Weaver and W. E. Geiger, *J. Am. Chem. Soc.*, 1989, **111**, 7084; W. E. Geiger, *Acc. Chem. Res.*, 1995, **28**, 351.
13 V. S. Leong and N. J. Cooper, *J. Am. Chem. Soc.*, 1988, **110**, 2644; J. A. Corella II and N. J. Cooper, *J. Am. Chem. Soc.*, 1990, **112**, 2832; R. L. Thompson, S. J. Geib and N. J. Cooper, *J. Am. Chem. Soc.*, 1991, **113**, 8961.
14 V. S. Leong and N. J. Cooper, *Organometallics*, 1988, **7**, 2058.
15 C. Bianchini, K. G. Caulton, C. Chardon, O. Eisenstein, K. Folting, J. J. Johnson, A. Meli, M. Peruzzini, D. J. Rauscher, W. E. Streib and F. Vizza, *J. Am. Chem. Soc.*, 1991, **113**, 5127; C. Bianchini, K. G. Caulton, K. Folting, A. Meli, M. Peruzzini, A. Polo and F. Vizza, *J. Am. Chem. Soc.*, 1992, **114**, 7290; C. Bianchini, P. Frediani, M. Graziani, J. Kaspar, A. Meli, M. Peruzzini and F. Vizza, *Organometallics*, 1993, **12**, 2886; C. Bianchini, M. Graziani, J. Kaspar, A. Meli and F. Vizza, *Organometallics*, 1994, **13**, 1165; C. Bianchini, K. G. Caulton, C. Chardon, M. L. Doublet, O. Eisenstein, S. A. Jackson, T. J. Johnson, A. Meli, M. Peruzzini, W. E. Streib, A. Vacca and F. Vizza, *Organometallics*, 1994, **13**, 2010.
16 J. Müller, P. E. Gaede and K. Qiao, *J. Organomet. Chem.*, 1994, **480**, 213.
17 J. Müller, P. E. Gaede and K. Qiao, *Angew. Chem., Int. Ed. Engl.*, 1993, **32**, 1697; J. Müller, C. Hirsch, K. Qiao and K. Ha, *Z. Anorg. Allg. Chem.*, 1996, **622**, 1441.
18 E. L. Muetterties, J. R. Bleeke and E. J. Wucherer, *Chem. Rev.*, 1982, **82**, 499.
19 D. Braga, P. J. Dyson, F. Grepioni and B. F. G. Johnson, *Chem. Rev.*, 1994, **94**, 1585.
20 B. F. G. Johnson, P. J. Dyson and C. M. Martin, *J. Chem. Soc., Dalton Trans.*, 1996, 2395.
21 E. Maslowsky, jun., *J. Chem. Educ.*, 1993, **70**, 980.
22 H. Wadepohl, *Angew. Chem., Int. Ed. Engl.*, 1992, **31**, 247.
23 M. A. Gallop, B. F. G. Johnson, J. Keeler, J. Lewis, S. J. Heyes and C. M. Dobson, *J. Am. Chem. Soc.*, 1992, **114**, 2510.
24 S. T. Belt, M. Helliwell, W. D. Jones, M. G. Partridge and R. N. Perutz, *J. Am. Chem. Soc.*, 1993, **115**, 1429.
25 T. W. Bell, M. Helliwell, M. G. Partridge and R. N. Perutz, *Organometallics*, 1992, **11**, 1911.
26 J. J. Barker, A. G. Orpen, A. J. Seeley and P. L. Timms, *J. Chem. Soc., Dalton Trans.*, 1993, 3097.
27 A. Martín, A. G. Orpen, A. J. Seeley and P. L. Timms, *J. Chem. Soc., Dalton Trans.*, 1994, 2251.
28 C. Aspley, C. L. Higgitt, C. Long and R. N. Perutz, unpublished work.
29 P. Hofmann and G. Unfried, *Chem. Ber.*, 1992, **125**, 659.
30 M. K. Whittlesey, R. N. Perutz and M. H. Moore, *Chem. Commun.*, 1996, 787.
31 A. H. Klahn, M. H. Moore and R. N. Perutz, *J. Chem. Soc., Chem. Commun.*, 1992, 1699.
32 M. Aizenberg and D. Milstein, *Science*, 1994, **265**, 359; M. Aizenberg and D. Milstein, *J. Am. Chem. Soc.*, 1995, **117**, 8674.
33 J. L. Kiplinger and T. G. Richmond, *Chem. Commun.*, 1996, 1115.
34 J. L. Kiplinger, T. G. Richmond and C. E. Osterberg, *Chem. Rev.*, 1994, **94**, 373.
35 C. K. Johnson, ORTEP, Report ORNL-5138, Oak Ridge National Laboratory, Oak Ridge, TN, 1976.
36 A. E. Derome, *Modern NMR Techniques for Chemistry Research*, Pergamon, Oxford, 1988.
37 C. L. Perrin and T. J. Dwyer, *Chem. Rev.*, 1990, **90**, 935.
38 R. R. Ernst, G. Bodenhausen and A. Wokaun, *Principles of Nuclear Magnetic Resonance in One and Two Dimensions*, Oxford University Press, New York, 1987.
39 B. E. Mann, in *Comprehensive Organometallic Chemistry*, eds. G. Wilkinson, F. G. A. Stone and E. W. Abel, Pergamon, Oxford, 1982, vol. 3, ch. 20.
40 C. L. Perrin and R. K. Gipe, *J. Am. Chem. Soc.*, 1984, **106**, 4036; C. L. Perrin, *J. Magn. Reson.*, 1989, **82**, 619; E. W. Abel, T. P. J. Coston, K. G. Orrell, V. Šik and D. Stephenson, *J. Magn. Reson.*, 1986, **70**, 34; I. Bányai, J. Glaser, K. Micskei, I. Tóth and L. Zékány, *Inorg. Chem.*, 1995, **34**, 3785; Z. Szabó and J. Glaser, *Magn. Reson. Chem.*, 1995, **33**, 20.
41 S. Macura and R. R. Ernst, *Mol. Phys.*, 1980, **41**, 95; G. Bodenhausen and R. R. Ernst, *J. Am. Chem. Soc.*, 1982, **104**, 1304.
42 R. Ramachandran, C. T. G. Knight, R. J. Kirkpatrick and E. Oldfield, *J. Magn. Reson.*, 1985, **65**, 136.
43 S. D. Ittel and J. A. Ibers, *Adv. Organomet. Chem.*, 1976, **14**, 33.
44 R. Cramer, J. B. Kline and J. D. Roberts, *J. Am. Chem. Soc.*, 1969, **91**, 2519; L. J. Guggenberger and R. Cramer, *J. Am. Chem. Soc.*, 1972, **94**, 3779.
45 O. J. Curnow, R. P. Hughes and A. L. Rheingold, *J. Am. Chem. Soc.*, 1992, **114**, 3153; O. J. Curnow, R. P. Hughes, E. N. Mairs and A. L. Rheingold, *Organometallics*, 1993, **12**, 3102.
46 I. Bach, K-R. Pörschke, R. Goddard, C. Kopiske, C. Krüger, A. Rufinska and K. Seevogel, *Organometallics*, 1996, **15**, 4959.

47 D. M. P. Mingos, in *Comprehensive Organometallic Chemistry*, eds. G. Wilkinson, F. G. A. Stone and E. W. Abel, Pergamon, Oxford, 1982, vol. 3, ch. 19.
48 B. E. R. Schilling, R. Hoffmann and D. L. Lichtenberger, *J. Am. Chem. Soc.*, 1979, **101**, 585.
49 T. A. Albright, R. Hoffmann, J. C. Thibeault and D. L. Thorn, *J. Am. Chem. Soc.*, 1979, **101**, 3801; T. A. Albright, *Acc. Chem. Res.*, 1982, **15**, 149; M. Mlekuz, P. Bougeard, B. G. Sayer, M. J. McGlinchey, C. A. Rodger, M. R. Churchill, J. W. Ziller, S-K. Kang and T. A. Albright, *Organometallics*, 1986, **5**, 1656.
50 M. Elian and R. Hoffmann, *Inorg. Chem.*, 1975, **14**, 1058; R. Hoffmann, *Angew. Chem., Int. Ed. Engl.*, 1982, **21**, 711.
51 J. A. Timney, *Inorg. Chem.*, 1979, **18**, 2502.
52 R. J. Angelici, G. Facchin and M. M. Singh, *Synth. React. Inorg. Met.-Org. Chem.*, 1990, **20**, 275.
53 C. P. Casey and E. W. Rutter, *J. Am. Chem. Soc.*, 1989, **111**, 8917.
54 C. F. Barrientospenna, A. H. Klahnoliva and D. Sutton, *Organometallics*, 1985, **4**, 367.
55 F. W. B. Einstein, A. H. Klahnoliva, D. Sutton and K. G. Tyers, *Organometallics*, 1986, **5**, 53.
56 J. K. Hoyano and W. A. G. Graham, *Organometallics*, 1982, **1**, 783.
57 M. J. S. Dewar, *Bull. Soc. Chim. Fr.*, 1951, **18**, C79; J. Chatt and L. A. Duncanson, *J. Chem. Soc.*, 1953, 2339.
58 T. A. Albright, J. K. Burdett and M. H. Whangbo, *Orbital Interactions in Chemistry*, Wiley-Interscience, New York, 1985.
59 S. Aime and L. Milone, *Prog. Nucl. Magn. Reson. Spectrosc.*, 1977, **11**, 183.
60 B. de Klerk-Engels, J. G. P. Delis, J.-M. Ernsting, C. J. Elsevier, H.-W. Frühauf, D. J. Stufkens, K. Vrieze, K. Goubitz and J. Fraanje, *Inorg. Chim. Acta*, 1995, **240**, 273.
61 K. Morokuma and W. T. Borden, *J. Am. Chem. Soc.*, 1991, **113**, 1912.
62 R. B. Woodward and R. Hoffmann, *The Conservation of Orbital Symmetry*, Academic Press, New York, 1970.
63 J. Browning, M. Green, B. R. Penfold, J. L. Spencer and F. G. A. Stone, *J. Chem. Soc., Chem. Commun.*, 1973, 31; J. Browning, C. S. Cundy, M. Green and F. G. A. Stone, *J. Chem. Soc. A*, 1971, 448; J. Browning, M. Green, J. L. Spencer and F. G. A. Stone, *J. Chem. Soc., Dalton Trans.*, 1974, 97.
64 C. D. Tagge and R. G. Bergman, *J. Am. Chem. Soc.*, 1996, **118**, 6908.
65 C. Amman, P. Meier and A. E. Merbach, *J. Magn. Reson.*, 1982, **46**, 319; A. L. Van Geet, *Anal. Chem.*, 1970, **42**, 679.
66 H. Günther, *NMR Spectroscopy: Basic Principles, Concepts and Applications in Chemistry*, Wiley, New York, 1995.
67 D. M. Haddleton, A. McCamley and R. N. Perutz, *J. Am. Chem. Soc.*, 1988, **110**, 1810.
68 TEXSAN-TEXRAY Structure Analysis Package, Molecular Structure Corporation, The Woodlands, TX, 1985.
69 G. M. Sheldrick, SHELXL 93, Program for the Refinement of Crystal Structures, University of Göttingen, 1995.
70 (*a*) E. O. Fischer and W. Fellmann, *J. Organomet. Chem.*, 1963, **1**, 191; (*b*) C. P. Casey, M. A. Andrews, D. R. McAlister and J. E. Rinz, *J. Am. Chem. Soc.*, 1980, **102**, 1927.

Received 2*nd December* 1996; *Paper* 6/08135E